Annals of Operations Research
https://doi.org/10.1007/s10479-026-07275-x

ORIGINAL RESEARCH

Generalized Ordinal Priority Approach with small-sample incomplete preference learning for multi-attribute decision-making

Renlong Wang[1]

Received: 20 April 2025 / Accepted: 8 May 2026

Abstract

Ordinal Priority Approach (OPA) is an optimization-based multi-attribute decision-making method that determines the weights of experts, attributes, and alternatives from ordinal rankings. To clarify its underlying structure, I first develop an equivalent formulation of OPA by mapping alternatives to rank indices. The resulting constraints explicitly involve rank order centroid (ROC) weights, showing that OPA can be interpreted as maximizing a weight disparity scalar in a ROC-weighted normalized decision space. Building on this equivalence, I then propose Generalized Ordinal Priority Approach (GOPA), an estimate-then-optimize bilevel framework that replaces fixed ROC utilities with utilities learned from partial preference information. At the lower level, I instantiate GOPA with minimum relative utility entropy (GOPA-RUE), in which expert-attribute marginal utility densities are elicited by combining a reference utility density (e.g., risk-aversion or S-shaped structures) with moment-type deterministic comparison constraints. Under this formulation, the optimal density admits an exponential-tilting, breakpoint-induced piecewise form and can be computed through a tractable linear-system reformulation, while regularized (nonnegative) least-squares corrections are used to address elicitation inconsistencies. At the upper level, once utilities have been elicited, the decision weights and the optimal disparity scalar admit closed-form solutions, yielding an efficient algorithm. Based on these results, I further establish the decomposability of the optimal weights and provide sensitivity analyses with respect to constraint, ranking, and utility perturbations. Finally, a Zhengzhou 7.20 emergency supplier selection study, together with ablation and perturbation experiments, demonstrates the flexibility and robustness of GOPA-RUE under limited and noisy preference information.

Keywords Multi-attribute decision-making · Incomplete preference learning · Bilevel optimization · Generalized Ordinal Priority Approach

✉ Renlong Wang
13127073530@163.com

[1] School of Emergency Management Science and Engineering, University of Chinese Academy of Sciences, Beijing 100049, China

Published online: 29 May 2026

1 Introduction

In the past decades, multi-attribute decision-making (MADM) has been regarded as an effective tool for addressing complex decision problems, adept at tackling challenges such as objective conflicts, data diversity and high uncertainty (Resende et al., 2023). A classical problem involves selecting an optimal alternative or obtaining a global ranking from a set of alternatives under multiple attributes based on multi-expert opinions. More specifically, for a given expert set $\mathcal{I}$, attribute set $\mathcal{J}$, and alternative set $\mathcal{K}$, the evaluation score V_k of alternative $k \in \mathcal{K}$ can be determined by a mapping $F : \mathbb{R}^{|\mathcal{I}|\times|\mathcal{J}|} \mapsto \mathbb{R}$ that has an associated collection of the weights for experts w_i and attributes w_j:

$$V_k = F(\boldsymbol{v}_k) = \sum_{i\in\mathcal{I}} \sum_{j\in\mathcal{J}} w_i w_j v_{ijk},$$

where v_{ijk} is the performance score of alternative k under attribute j given by expert i. Typically, much of the research is based on precise weights of experts and attributes obtained through sophisticated heuristic methods (Zayat et al., 2023). Meanwhile, some studies have emerged to elicit weight through incomplete information, which is often referred to as imprecise or partial preference information, to address challenges such as inadequate data and domain knowledge, and limitations in DMs' attention and information processing capabilities within the time constraints (Ahn, 2024). Of course, if DMs can provide all the information required to solve the MADM problems, prior (sophisticated) methods based on precise data is recommended.

1.1 Related literature

Current methods for weight elicitation under incomplete preference information mainly fall into two categories: optimization-based approaches and extreme point-based approaches. The former aims to model and solve the optimal set of weights under the constraints of incomplete preference information (Kim and Ahn, 1999; Malakooti, 2000; Wang et al., 2007). Conversely, the latter capitalizes on the extreme points within incomplete data to ascertain weights (Ahn, 2015, 2017, 2024). Some research have suggested an evolving synthesis of these two approaches. Within optimization-based approaches, the DEA-based preference voting model, which incorporates partial preference information in a ratio scale, is prevalently employed (Wang et al., 2007). Correspondingly, Ahn (2017) derives a closed-form expression for the optimal solution of the DEA-based preference voting model by imposing the weight constraints from the extreme points of partial preference information. Furthermore, Ahn (2024) derives a dual problem of linear programming to obtain closed-form solutions and establish a strict ranking of extremal points of attribute weights. Additionally, a prevalent weight elicitation approach involves rank-based surrogate weights for weight elicitation, where each rank-based surrogate weight is uniquely represented by a set of extreme points (Burk and Nehring, 2023). Llamazares (2024) proposes explicit expressions of weights based on various simplex centroids in ranking voting frameworks inspired by specific simplex centroids of rank order centroid (ROC) weights.

Ordinal Priority Approach (OPA) is an optimization-based value function method for addressing the MADM under incomplete information (Ataei et al., 2020). OPA derives weights from a normalized weight space with ordinal preference using linear programming, simultaneously determining weights for experts, attributes, and alternatives. OPA is applicable to both group and individual decision-making. Compared to typical inputs in other

MADM methods, such as cardinal values and pairwise comparisons, ordinal data is more accessible to obtain and more stable (Wang, 2025). Unlike traditional methods, OPA avoids the need for data standardization, expert opinion aggregation, and prior weight acquisition. Additionally, various extensions of OPA have emerged, such as fuzzy OPA (Sadeghi et al., 2023; Zhao et al., 2024), rough OPA (Du et al., 2023; Kucuksari et al., 2023), grey OPA (Mahmoudi et al., 2021), robust OPA (Mahmoudi et al., 2022a; Mao and Wang, 2026), and distributionally robust OPA (Cui et al., 2025b) for handling decision data uncertainty, DGRA-OPA (Wang, 2024) and TOPSIS-OPA (Mahmoudi et al., 2022b) for addressing large-scale group decision-making, partial OPA (Wang et al., 2025) for managing potential Pareto dominance, and DEA-OPA (Mahmoudi et al., 2022a; Cui et al., 2025a) for relative efficiency analysis with subjective preference. Consequently, OPA has garnered increasing attention recently and has been applied across various domains, including sustainable transportation evaluation (Pamucar et al., 2022), supplier evaluation (Mahmoudi et al., 2021; Mahmoudi and Javed, 2022), blockchain analysis (Sadeghi et al., 2023; Zhao et al., 2024), project portfolio selection (Mahmoudi et al., 2022a), and emergency recovery planning (Wang, 2024).

Existing approaches to weight elicitation under incomplete preference information, particularly OPA, largely neglect the role of DMs' risk preferences in weight assignment, implicitly assuming homogeneous risk attitudes. OPA has yet to examine how scale distortions arising from heterogeneous risk preferences may affect decision outcomes. Moreover, despite its practical appeal, OPA has received limited scrutiny regarding its fundamental properties. The absence of structural analysis constrains the effective integration of partial preference information, such as ratio scales and absolute differences, beyond purely ordinal inputs.

1.2 Contributions

Building on the fundamental properties of OPA established herein, I propose Generalized Ordinal Priority Approach (GOPA) to accommodate small-sample incomplete preference learning, extending the ROC weights for ranked alternatives in OPA to a more flexible utility structure. GOPA adopts an estimate-then-optimize bilevel framework: the first stage conducts utility preference learning via a minimum cross-utility entropy estimator under a specified preference context, and the second stage optimizes decision weights based on the inferred utilities. A central component of GOPA is the design of a preference context that embeds risk preferences, together with an analysis of the cross-utility entropy minimization problem, which enables a tractable formulation. The main contributions are summarized as follows:

- *Modeling.* I reinterpret OPA by deriving an equivalent rank-index formulation that uncovers its intrinsic link to ROC-type surrogate utilities, thereby providing a transparent structural account of OPA's rank-weight mapping and the role of multiplicative ranking parameters (Proposition 1). Motivated by this equivalence, I propose GOPA, which replaces fixed ROC utilities with a flexible utility representation learned from small-sample, incomplete preference information. GOPA is formulated as an estimate-then-optimize bilevel model: the lower level reconstructs marginal utilities under a unified preference context, and the upper level optimizes decision weights based on the elicited utilities (Equation (8)). A key innovation is the preference context design, which simultaneously incorporates (i) reference utility structures (e.g., risk-preference or S-shaped utilities) and (ii) moment-type partial preference constraints that unify ratio-scale, absolute-difference, and lower-bound elicitation within a single framework (Definition 1 and Example 1). This construction extends OPA beyond rank-driven ROC transformations and enables utility reconstruction across heterogeneous attributes and experts, while remaining implementable in the absence of a reference structure via utility-entropy maximization (Corollary 1).

- *Theory.* I establish tractable structural results for both levels of GOPA and their interaction. For lower-level preference learning, I characterize the optimal marginal utility density under minimum relative utility entropy as an exponential-tilting form with breakpoint-induced piecewise structure (Theorem 1), and show that the solution reduces to a linear system over interval masses (Proposition 2). I prove that the elicitation strategy induces a full-column-rank matrix, ensuring identifiability and well-posed regularized estimation (Lemma 1), and demonstrate how reference structures govern local risk attitudes within elicited intervals (Corollary 2). For the upper level, I derive closed-form solutions for the optimal weight disparity scalar and decision weights given reconstructed utilities (Theorem 2). I further establish a decomposability property: optimal weights factor into rank-reciprocal components for experts and attributes and a utility-driven component for alternatives. This result rigorously justifies the multiplicative ranking mechanism in OPA and identifies OPA as a special case obtained by substituting ROC utilities (Corollary 3). Finally, I provide sensitivity results with respect to constraint and ranking perturbations, yielding explicit bounds and robustness regions for the optimal solutions (Theorem 3 and Corollary 4).
- *Algorithm.* Building on these structural results, I develop an efficient procedure for GOPA-RUE with polynomial complexity in the number of elicited breakpoints and decision dimensions (Algorithm 1). The algorithm integrates (i) a regularized least-squares solver for lower-level utility reconstruction, augmented with feasibility checks and a nonnegative regularized correction to address noisy or inconsistent constraints (Propositions 3 and the subsequent nonnegativity formulation), and (ii) closed-form aggregation for upper-level weight optimization (Theorem 2). The resulting pipeline is computationally stable under limited and imperfect preference inputs, preserves interpretability through explicit decomposition, and produces globally normalized weights at the expert, attribute, and alternative levels.

1.3 Organization

The remainder of this paper is organized as follows: Section 2 presents the preliminaries of OPA. Section 3 proposes an equivalent formulation of OPA and further proposes the unified framework of GOPA. Section 4 introduces GOPA with minimum relative utility entropy (GOPA-RUE). Section 5 demonstrates GOPA-RUE through a numerical experiment on emergency supplier selection during the 7.20 mega-rainstorm disaster in Zhengzhou, China. Section 6 concludes this study and outlines future directions.

2 Ordinal Priority Approach

Consider a classical MADM setting that DM needs to determine the optimal alternative from a finite set of alterantives $\mathcal{K} = \{1, 2, \ldots, K\}$, based on their performance across J attributes, $\mathcal{J} = \{1, 2, \ldots, J\}$, as assessed by I experts, $\mathcal{I} = \{1, 2, \ldots, I\}$. OPA uses ranking data as input when acquiring objective data or subjective information, represented by evaluation scores or linguistic values, is challenging. For OPA, DM initially assigns a rank t_i to each expert $i \in \mathcal{I}$ based on factors such as work experience, educational background, and organizational structure. Each expert $i \in \mathcal{I}$ then independently ranks each attribute $j \in \mathcal{J}$ as s_{ij}

and each alternative $k \in \mathcal{K}$ on any attribute $j \in \mathcal{J}$ as r_{ijk}.Following standard conventions, the highest rank is assigned as 1, the next as 2, and so on. In OPA, each expert acts as an independent individual, offering evaluations without group deliberation, which means all rankings reflect their personal preferences.

To simplify the discussion, I first define the following sets:

$$\begin{aligned}
\mathcal{X}^1 &:= \left\{(i, j, k, l) \in \mathcal{I} \times \mathcal{J} \times \mathcal{K} \times \mathcal{K} : r_{ijl} = r_{ijk} + 1, r_{ijk} \in [K-1]\right\}, \\
\mathcal{X}^2 &:= \left\{(i, j, k) \in \mathcal{I} \times \mathcal{J} \times \mathcal{K} : r_{ijk} = K\right\}, \\
\mathcal{X} &:= \{(i, j, k) \in \mathcal{I} \times \mathcal{J} \times \mathcal{K}\}, \\
\bar{\mathcal{X}} &:= \{(i, j) \in \mathcal{I} \times \mathcal{J}\}.
\end{aligned}$$

Intuitively, $\mathcal{X}^1$ captures alternatives with consecutive rankings for each attribute and expert, whereas $\mathcal{X}^2$ collects alternatives ranked last for each attribute and expert. Moreover, $\mathcal{X} = \mathcal{X}^1 \cup \mathcal{X}^2$ represents all expert attribute alternative combinations, and $\bar{\mathcal{X}}$ represents all expert attribute pairs. Let $k^{(r_{ijk})}$ represent alternative k ranked r_{ijk} on attribute j by expert i with the weight of w_{ijk}. Essentially, OPA is a value function method; however, to maintain consistency with the original literature, I continue to use the term "weight." For any $(i, j) \in \bar{\mathcal{X}}$, alternatives with higher rankings dominate those with lower rankings:

$$\begin{aligned}
&l^{(r_{ijl})} \prec k^{(r_{ijk})} \Leftrightarrow w_{ijl} < w_{ijk}, && \forall (i, j, k, l) \in \mathcal{X}^1, \\
&\emptyset \prec k^{(r_{ijk})} \Leftrightarrow 0 < w_{ijk}, && \forall (i, j, k) \in \mathcal{X}^2.
\end{aligned} \tag{1}$$

Without loss of generality, assume that the weights are in the normalized weight space:

$$\mathcal{W} := \left\{ \boldsymbol{w} \in \mathbb{R}^{\mathcal{X}} : \sum_{i \in \mathcal{I}} \sum_{j \in \mathcal{J}} \sum_{k \in \mathcal{K}} w_{ijk} = 1,\ w_{ijk} \geq 0,\ \forall (i, j, k) \in \mathcal{X} \right\}.$$

To incorporate the impact of expert preference on the weight disparity of each pair of alternatives with consecutive rankings, OPA multiplies both sides of the inequalities in Equation (1) by the ranking parameters:

$$\begin{aligned}
&t_i s_{ij} r_{ijk} (w_{ijk} - w_{ijl}) > 0, && \forall (i, j, k, l) \in \mathcal{X}^1, \\
&t_i s_{ij} r_{ijk} (w_{ijk}) > 0, && \forall (i, j, k) \in \mathcal{X}^2.
\end{aligned} \tag{2}$$

Equation (2) describes the marginal utility of weight increments or disparities derived from alternative ranking under each attribute and expert. Intuitively, the unconventional manipulation that multiplies the weight disparities of consecutively ranked alternatives by the rankings of experts, attributes, and alternatives suggests that as rankings increase, the marginal effect of weight disparity between consecutive alternatives diminishes. The rationality for this is demonstrated in this study by deriving the decomposability of the OPA weights (Theorem 2 and Corollary 3), linking the results to commonly used ranking-based surrogate weights in decision theory.

In the normalized weight space, any point within the polyhedron satisfying the conditions of Equation (2) aligns with expert preferences. Therefore, some studies offer a uniform distribution of marginal effects of all weight increments to accommodate every expert preferences without adding extra information (Sütçü, 2022). However, in the practical decision-making process, DMs are inclined to pursue the most robust decision weights that reflect expert preferences while demonstrating maximum disparities, which is common the MADM methods such as ROR and non-additive capacity identification (Greco et al., 2008; Timonin, 2013).

Thus, OPA, proposed by Ataei et al. (2020), seeks to maximize weight disparities that reflect expert preferences within the normalized weight space:

$$
\begin{aligned}
\text{[OPA-I]} \quad & \max_{\boldsymbol{w}, z} z, \\
& \text{s.t. } z \leq t_i s_{ij} r_{ijk} (w_{ijk} - w_{ijl}), && \forall (i, j, k, l) \in \mathcal{X}^1, \\
& \quad z \leq t_i s_{ij} r_{ijk} (w_{ijk}), && \forall (i, j, k) \in \mathcal{X}^2, \\
& \quad \sum_{i \in \mathcal{I}} \sum_{j \in \mathcal{J}} \sum_{k \in \mathcal{K}} w_{ijk} = 1, \\
& \quad w_{ijk} \geq 0 && \forall (i, j, k) \in \mathcal{X}.
\end{aligned} \tag{3}
$$

where $z \in \mathbb{R}$ represents a weight disparity scalar. After solving Equation (3) for the optimal solutions $(z^*, \boldsymbol{w}^*)$, the weight of experts, attributes, and alternatives, denoted as $W_i^{\mathcal{I}}$, $W_j^{\mathcal{J}}$, and $W_k^{\mathcal{K}}$, respectively, are given by

$$
\begin{aligned}
W_i^{\mathcal{I}} &= \sum_{j \in \mathcal{J}} \sum_{k \in \mathcal{K}} w_{ijk}^*, && \forall i \in \mathcal{I}, \\
W_j^{\mathcal{J}} &= \sum_{i \in \mathcal{I}} \sum_{k \in \mathcal{K}} w_{ijk}^*, && \forall j \in \mathcal{J}, \\
W_k^{\mathcal{K}} &= \sum_{i \in \mathcal{I}} \sum_{j \in \mathcal{J}} w_{ijk}^*, && \forall k \in \mathcal{K}.
\end{aligned} \tag{4}
$$

In individual decision-making, OPA-I can be formulated without the parameters and constraints associated with DMs. When experts deem certain attributes or alternatives irrelevant, they are excluded from the decision-making process, along with their corresponding decision variables and constraints. When two alternatives have identical rankings for a specific expert and attribute, their weight difference is zero.

3 Equivalent formulation and generalization of ordinal priority approach

3.1 Equivalent formulation of ordinal priority approach

This section develops an equivalent formulation of OPA-I and examines its structural implications, which form the basis for the subsequent analysis.

Without loss of generality, I first map the alternative index k in w_{ijk} to the rank index r based on their positions in r_{ijk} and define a set:

$$\mathcal{Y} := \{(i, j, r) \in \mathcal{I} \times \mathcal{J} \times \mathcal{R} : \ \mathcal{R} = \{1, \ldots, R\}, \ R = K\}.$$

Proposition 1 *OPA-I admits the following equivalent formulation:*

$$
\begin{aligned}
\textit{[OPA-II]} \quad & \max_{\bar{\boldsymbol{w}}, z} z, \\
& \text{s.t. } \left(\sum\nolimits_{h=r}^{R} \frac{1}{h} \right) z \leq t_i s_{ij} \bar{w}_{ijr}, && \forall (i, j, r) \in \mathcal{Y}, \\
& \quad \sum_{i \in \mathcal{I}} \sum_{j \in \mathcal{J}} \sum_{r \in \mathcal{R}} \bar{w}_{ijr} = 1, \\
& \quad \bar{w}_{ijr} \geq 0, && \forall (i, j, r) \in \mathcal{Y},
\end{aligned} \tag{5}
$$

where z is the weight disparity scalar, and $\bar{w}_{ijr}$ is the weight of alternative ranked r on attribute j by expert i. The feasible set of OPA-II is nonempty, the objective function is bounded above, and an optimal solution exists.

The dual problem of OPA-II is formulated as follows:

$$\begin{aligned} \min_{\boldsymbol{\lambda},\lambda_0} \; & \lambda_0, \\ \text{s.t.} \; & t_i s_{ij} \lambda_{ijr} \le \lambda_0, & \forall (i,j,r) \in \mathcal{Y}, \\ & \sum_{i\in\mathcal{I}} \sum_{j\in\mathcal{J}} \sum_{r\in\mathcal{R}} \left(\sum\nolimits_{h=r}^{R} \frac{1}{h} \right) \lambda_{ijr} = 1, \\ & \lambda_{ijr} \ge 0, & \forall (i,j,r) \in \mathcal{Y}, \end{aligned} \tag{6}$$

and strong duality holds.

After solving OPA-II, the optimal weight $\bar{w}^*_{ijr}$ is assigned to the alternative ranked r_{ijk} under each expert-attribute pair $(i, j) \in \bar{\mathcal{X}}$. Note that the left-hand side of the inequality constraints in OPA-II can be written as

$$\sum_{h=r}^{R} \frac{1}{h} = R\, U_r^{\mathrm{ROC}}, \quad \forall r \in \mathcal{R},$$

which corresponds to the rank order centroid (ROC) weight associated with rank r scaled by the number of alternatives. Accordingly, Proposition 1 shows that OPA-II admits an interpretation as eliciting the maximum weight disparity scalar based on ROC weights within a normalized decision space. This formulation is therefore equivalent to maximizing weight disparities while preserving the ranking preferences specified in OPA-I.

For clarity of the subsequent discussions, rewrite OPA-II as

$$\max_{\bar{\boldsymbol{w}}\in\bar{\mathcal{W}},z} \left\{ z : \boldsymbol{f}(z) \le \boldsymbol{g}(\boldsymbol{w}) \right\}, \tag{7}$$

where $[\boldsymbol{f}(z)]_{ijr} = f_{ijr}(z) = RU_r^{ROC} z$ and $[\boldsymbol{g}(\boldsymbol{w})]_{ijr} = g_{ijr}(w_{ijr}) = t_i s_{ij} \bar{w}_{ijr}$ for all $(i, j, r) \in \mathcal{Y}$, and

$$\bar{\mathcal{W}} := \left\{ \bar{\boldsymbol{w}} \in \mathbb{R}^{\mathcal{Y}} : \sum_{i\in\mathcal{I}} \sum_{j\in\mathcal{J}} \sum_{r\in\mathcal{R}} \bar{w}_{ijr} = 1,\; \bar{w}_{ijr} \ge 0, \forall (i,j,r) \in \mathcal{Y} \right\}.$$

3.2 Generalized Ordinal Priority Approach

The core idea of GOPA is to extend the original ROC weights for ranked alternatives in OPA-II into a more adaptable utility structure derived from customized partial preference information. In this context, the utilities for ranked alterantives under different experts and attributes are treated as uncertainty parameters. The partial preference information and reference utility structure provided by DMs can serve as side information for deriving utilities. Denote by $U_{ij} : (0, R] \to \mathbb{R}$ the marginal utility function for any $(i, j) \in \bar{\mathcal{X}}$ defined over the interval $(0, R]$, with a finite number of non-differentiable breakpoints at

$$0 = r_0 < \cdots < r_{C_{ij}} = R,$$

where $\mathcal{C}_{ij} := \{1, \ldots, C_{ij}\}$. Without loss of generality, assume that the marginal utility function $U(x)$ is nondecreasing, lower semi-continuous, and normalized within $[0, 1]$ with the support set:

$$\mathcal{U} := \left\{ U \in \mathscr{U} : \int_0^R u(x)\mathrm{d}x = 1 \right\},$$

where $\mathscr{U}$ represents the class of nondecreasing and lower semi-continuous marginal utility functions and $u(x)$ is the marginal utility density function of $U(x)$.

This study introduces an estimate-then-optimize bilevel optimization framework for GOPA. In this framework, the lower-level problem estimates the marginal utility density functions of ranked alternatives across all experts and attributes based on partial preference information, while the upper-level problem optimizes the corresponding decision weights. Let $U_{ijr} = \int_0^{R-r+1} u_{ij}(x)\,\mathrm{d}x$ for all $(i, j, r) \in \mathcal{Y}$, where $u_{ij}(x)$ denotes the marginal utility density function associated with expert i and attribute j. Let $\mathcal{P}_{ij}$ denote the feasible set induced by partial preference information, and let $v_{ij} : (0, R] \to \mathbb{R}$ be a reference marginal density function for each $(i, j) \in \bar{\mathcal{X}}$. Under this setting, the unified framework of GOPA can be formulated as the following bilevel optimization problem:

$$\begin{aligned}
&[\text{GOPA}] \quad \max_{\bar{\boldsymbol{w}} \in \bar{\mathcal{W}},\, z} \quad z, && \text{(Upper level: optimize)}\\
&\qquad \text{s.t. } \boldsymbol{f}(z) \le \boldsymbol{g}(\bar{\boldsymbol{w}}, \boldsymbol{U}^*),\\
&\qquad u_{ij}^*(x) = \underset{u_{ij} \in \mathcal{P}_{ij} \cap \mathcal{U}}{\arg\min}\; h\left(u_{ij}(x),\; v_{ij}(x)\right), \ \forall (i, j) \in \bar{\mathcal{X}}, && \text{(Lower level: estimate)}
\end{aligned} \tag{8}$$

Accordingly, the key to the success of GOPA depends on the design of preference contexts that embed reference utility structures and partial preference information, and on the selection of an appropriate lower-level preference learning estimator.

The GOPA framework generalizes utility representations for ranked alternatives and extends to multiple data types, including objective measurements, evaluation scores, and expert semantic assessments. For each data type, a suitable utility function satisfies monotonicity and normalization, mapping attribute specific performance to comparable utility values and enabling cross attribute comparison.

4 Generalized ordinal priority approach with minimum relative utility entropy

This section specifies a concrete instantiation of the unified GOPA framework by adopting the minimum relative utility entropy estimator for the lower-level preference learning, referred to as GOPA-RUE. Under this specification, I derive a tractable reformulation of the resulting problem and develop an associated computational framework.

4.1 Utility entropy

The concept of utility entropy was first introduced by Abbas (2006) based on the utility increment vector, drawing an analogy to the probability mass function in probability theory. Consequently, utility entropy measures the uncertainty associated with a utility random variable. It adheres to the axioms of Von Neumann and Morgenstern's expected utility theory while satisfying the fundamental independence between utility and probability. Given the normative distinction between belief and preference, the utility value of a prospect is unaffected by the probability of its realization (Jose et al., 2008).

Let $U = (0, U_1, U_2, \ldots, U_{K-2}, 1)$ denote a utility vector with K elements. The corresponding discrete utility increment vector with $K-1$ elements is defined as

$$\Delta \boldsymbol{U} = (U_1 - 0, U_2 - U_1, \ldots, 1 - U_{K-2}) = (\Delta U_1, \Delta U_2, \ldots, \Delta U_{K-1}).$$

The utility entropy of this increment vector is defined as

$$H(\Delta \boldsymbol{U}) = -\sum_{k=1}^{K-1} \Delta U_k \log(\Delta U_k).$$

For the continuous case, with a utility density function $u(x)$ over the domain $[a, b]$, utility entropy is defined similarly to the discrete case:

$$h(u(x)) = -\int_a^b u(x) \ln(u(x)) \mathrm{d}x.$$

Abbas (2006) further defines the maximum utility entropy and minimum relative utility entropy, drawing an analogy between utility and probability. Given constraints that represent partial preference information, the maximum utility entropy formulation in the continuous case is

$$\begin{aligned} u^*(x) = \arg\max_{u(x)} \ & -\int_a^b u(x) \ln(u(x)) \mathrm{d}x, \\ \text{s.t.} \ & \int_a^b h_c(x) u(x) \mathrm{d}x = \mu_i, \qquad c = 1, \ldots, C, \\ & \int_a^b u(x) \mathrm{d}x = 1, \\ & u(x) \geq 0. \end{aligned} \tag{9}$$

The minimum relative utility entropy formulation, given a reference utility density $v(x)$, is obtained by replacing the objective of the maximum utility entropy formulation with

$$\min_{u(x)} h(u(x), v(x)) = \int_a^b u(x) \ln\left(\frac{u(x)}{v(x)}\right) \mathrm{d}x. \tag{10}$$

This study adopts relative utility entropy minimization for the lower level preference learning of GOPA, motivated by its flexibility with small sample inputs. The approach enables experts to provide sufficiently reliable decision information without stringent statistical data requirements, thereby reducing the decision making burden of DMs. Moreover, relative utility entropy minimization yields maximum likelihood estimates when the underlying distribution belongs to the exponential family, which is consistent with the reference utility density in the lower level problem of GOPA. In the absence of prior structural knowledge, it further reduces to utility entropy maximization, allowing utility elicitation based solely on partial preference information and addressing the challenge of accurately capturing DMs' utility structures. The latter two properties are demonstrated in the following analysis.

4.2 Preference context design

The preference context design in GOPA mainly includes two parts: reference utility structure construction and partial preference information characterization.

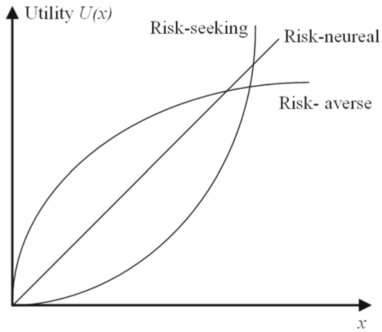

Fig. 1 Utility function and its risk behaviour

4.2.1 Reference utility structure construction

The reference utility structure in GOPA provides prior information for eliciting the utilities of ranked alternatives. The construction of reference utility structure is mainly based on selecting an appropriate utility function and extracting its utility density function. This study employs the risk preference utility function as the reference function for continuous prospects. Notably, the lack of reference utility information does not hinder the implementation of GOPA, which can still demonstrate favorable properties.

Abundant evidence demonstrates that risk preference significantly impacts practical decision-making processes, particularly in finance, economics, and decision science (Chen and Sim, 2024; Liesiö et al., 2023). It typically molds DMs' cognitive processing of information and ultimately guiding their inclination towards optimal solutions (Peng and Delage, 2024). The risk preference generally manifest as risk-seeking, risk-neutral, and risk-averse tendencies, which can be elucidated through utility functions. The behaviors of the risk-seeking, risk-neutral, and risk-averse utility functions exhibit concave, linear, and convex characteristics, respectively, as illustrated in Fig. 1.

Among the different risk preference utility functions, hyperbolic absolute risk aversion (HARA) has gained widespread application due to its generality (Xie et al., 2024). The HARA utility function is given by

$$V(x) = \frac{1}{1-\gamma}\left(\gamma\left(\beta + \frac{\alpha}{\gamma}x\right)^{1-\gamma} - 1\right),$$

with the utility density:

$$v(x) = \alpha\left(\beta + \frac{\alpha}{\gamma}x\right)^{-\gamma},$$

where α, β, and γ are given constants. The HARA utility function can be generalized to common utility function forms:

- when $\gamma = 0$, it reduces to a risk-neutral utility function;
- when $\beta = 0$ and $\gamma > 0$, it reduces to a constant relative risk-averse (CRRA) utility function;
- when $\gamma \to \pm\infty$, it reduces to a constant absolute risk aversion (CARA) utility function.

Besides the above risk preference utility functions with single feature, the prospect theory proposed by Tversky and Kahneman (1974) represents a significant approach to bridging the gap between normative theories and empirical behaviors. It suggests that decision-making is influenced by four factors: (1) outcome evaluation relative to a reference point; (2) losses have a more significant impact on DMs than gains; (3) increasing gains or losses weakens people's perceptions of them; (4) individuals exhibit probability distortion, tending to overweight small probabilities and underestimate large ones. These observations indicate that individuals exhibit risk aversion toward gains and risk-seeking toward losses. Thus, the utility functions based on prospect theory exhibit an S-shaped characteristic. Consistent with normative research practices, the possibility of any probability evaluation bias are disregarded in this study, focusing instead on how to incorporate information indicating specific shapes of utility functions (Armbruster and Delage, 2015). This study adopts a logistic function as the utility function with the S-shaped characteristic, given by

$$V(x) = \frac{1}{1+e^{-x}}.$$

We need further perform translation and stretching transformations to make it symmetric about point $(R/2, 0.5)$, i.e.,

$$V(x) = \frac{1}{1+e^{-(x-\frac{R}{2})}},$$

with the utility density:

$$v(x) = \frac{e^{-(x-\frac{R}{2})}}{(1+e^{-(x-\frac{R}{2})})^2}.$$

The choice of a reference utility structure in practice primarily depends on the available prior information. When the DMs' overall risk preference can be identified, monotonic risk preference utilities such as the HARA utility function can be adopted, with curvature parameters capturing risk seeking or risk aversion. When the decision process is strongly influenced by reference point effects or gain loss asymmetry, a logistic utility function with an S-shaped structure is more appropriate. If a DM is unable to clearly specify or justify an appropriate reference point, no reference-dependent specification is imposed. It should be emphasized that the identification of utility structures has been extensively studied in behavioral economics and decision theory. The focus of this study is instead to develop a general framework that can embed multiple reference utility structures, and thus the specific identification procedure is not discussed.

4.2.2 Preference information characterization

Partial preference information serves as the basis for constructing the feasible sets of marginal utility functions in the lower-level problems of GOPA. This section introduces a moment-type preference set for utility functions, which is highly generalizable and accommodates various forms of partial preference information in the current literature of decision analysis.

Definition 1 The set of utility functions satisfying the moment-type preference (MTP) is defined as

$$\mathcal{P} := \left\{ U \in \mathscr{U} : -\infty < \int_{\Theta} \phi_b(x) \mathrm{d}U(x) \le \beta_b, b = 1, \ldots, B \right\}, \tag{11}$$

where $\phi_b : \Theta \to \mathbb{R}$ is Lebesgue integrable function and β_b is some given constant for $b = 1, \ldots, B$.

The function ϕ_b and parameter β_b represent partial preference information, which varies across attributes and among different experts. The MTP set includes various forms of partial preference information with several sensible examples presented below.

Example 1 (Deterministic Utility Comparison) The preference information of deterministic utility comparison mainly includes ratio scales, absolute differences, lower bounds, and weak ordered relations. Consider two alternatives with performance values $\theta_1, \theta_2 \in \Theta$ on benefit-based attribute (i.e., the larger value is preferred), where $\theta_1 > \theta_2$. Ratio scale for deterministic utility comparison is commonly employed by pairwise comparison methods such as AHP, ANP, and BWM. The set of utility functions satisfying the ratio scale preference $\alpha > 1$ is expressed as

$$\mathcal{P}^{\text{rs}} := \left\{ U \in \mathscr{U} : \int_{\underline{\theta}}^{\theta_1} \mathrm{d}U(x) = \alpha \int_{\underline{\theta}}^{\theta_2} \mathrm{d}U(x) \right\}.$$

Absolute difference for deterministic utility comparison is typically used by the quasi-distance-based MADM methods such as TOPSIS, VIKOR, and EDAS. The set of utility functions satisfying the absolute difference preference β is expressed as

$$\mathcal{P}^{\text{ab}} := \left\{ U \in \mathscr{U} : \int_{\underline{\theta}}^{\theta_1} \mathrm{d}U(x) - \int_{\underline{\theta}}^{\theta_2} \mathrm{d}U(x) = \beta \right\}.$$

The set of utility functions satisfying the lower bound preference γ is expressed as

$$\mathcal{P}^{\text{lb}} := \left\{ U \in \mathscr{U} : \int_{\underline{\theta}}^{\theta_1} \mathrm{d}U(x) = \gamma \right\}.$$

The set of utility functions satisfying the weak ordered relation is expressed as

$$\mathcal{P}^{\text{wo}} := \left\{ U \in \mathscr{U} : \int_{\underline{\theta}}^{\theta_1} \mathrm{d}U(x) \geq \int_{\underline{\theta}}^{\theta_2} \mathrm{d}U(x) \right\}.$$

When $\alpha = 1$ and $\beta = 0$, $\mathcal{P}^{\text{rs}}$ and $\mathcal{P}^{\text{ab}}$ reduce to $\mathcal{P}^{\text{wo}}$, respectively. This suggests that weak ordered relations can be foundational for integrating other reliable partial preference information from DMs to approximate actual preferences.

By introducing the indicator function, I can rewrite the above sets into

$$\begin{aligned}
\mathcal{P}^{\text{rs}} &:= \left\{ U \in \mathscr{U} : \int_{\Theta} \left(\mathbf{1}_{(\underline{\theta},\theta_1]}(x) - \alpha \mathbf{1}_{(\underline{\theta},\theta_2]}(x) \right) \mathrm{d}U(x) = 0 \right\}, \\
\mathcal{P}^{\text{ab}} &:= \left\{ U \in \mathscr{U} : \int_{\Theta} \left(\mathbf{1}_{(\underline{\theta},\theta_1]}(x) - \mathbf{1}_{(\underline{\theta},\theta_2]}(x) \right) \mathrm{d}U(x) = \beta \right\}, \\
\mathcal{P}^{\text{lb}} &:= \left\{ U \in \mathscr{U} : \int_{\Theta} \mathbf{1}_{(\underline{\theta},\theta_1]}(x) \mathrm{d}U(x) = \gamma \right\}, \\
\mathcal{P}^{\text{wo}} &:= \left\{ U \in \mathscr{U} : \int_{\Theta} \left(\mathbf{1}_{(\underline{\theta},\theta_1]}(x) - \mathbf{1}_{(\underline{\theta},\theta_2]}(x) \right) \mathrm{d}U(x) \geq 0 \right\},
\end{aligned}$$

where $\mathbf{1}_{(\underline{\theta},\theta_1]}(\cdot)$ is the indicator function with domain $(\underline{\theta}, \theta_1] \in \Theta$. It is straightforward to unify the above set into a MTP set, with ϕ being constant within different intervals.

This study considers the MTP set based on the deterministic utility comparisons. Experts need only to provide sufficiently determined preference information, which forms the basis for personalized preference analysis. Since the marginal utility function is non-decreasing, the weak order relations always hold, and thus only ratio scales, absolute differences, and lower bounds need to be considered. Consequently, for any $(i, j) \in \bar{\mathcal{X}}$, the partial preference context for GOPA can be expressed as

$$\mathcal{P}_{ij} := \left\{ U_{ij} \in \mathscr{U} : -\infty < \int_0^R \phi_{b_{ij}}(x) \mathrm{d}U_{ij}(x) = \beta_{b_{ij}}, \forall b_{ij} \in \mathcal{B}_{ij} \right\}, \tag{12}$$

where $\phi_{b_{ij}}(x) = \mathbf{1}_{(0, r_{b_{ij}}]}(x) - \alpha \mathbf{1}_{(0, r_{b'_{ij}}]}(x)$ and $\mathcal{B}_{ij} = \{1, \ldots, B_{ij}\}$.

The MTP elicitation process is conducted incrementally. Upon eliciting a deterministic comparison b_{ij}, the associated comparison points are incorporated into the breakpoint set, i.e.,

$$\mathcal{C}_{ij} \leftarrow \mathcal{C}_{ij} \cup \{r_{b_{ij}}, r_{b'_{ij}}\}, \quad \forall\, b_{ij} \in \mathcal{B}_{ij}.$$

To limit the proliferation of induced segments, the first comparison is allowed to introduce two new breakpoints, whereas each subsequent comparison introduces at most one new breakpoint, satisfying

$$\left| \{r_{b_{ij}}, r_{b'_{ij}}\} \setminus \mathcal{C}_{ij} \right| \leq 1.$$

This strategy regulates the growth of the piecewise structure relative to the number of elicited MTP constraints, ensuring that the model dimensionality remains commensurate with the available preference information.

4.3 Reformulation

This section derives a tractable reformulation of GOPA-RUE and develops an associated computational framework through an analysis of its structural properties.

4.3.1 Lower-level estimation for preference utility

Consider the lower-level problem of GOPA-RUE that minimizes the relative utility entropy under the above discussed preference context for each $(i, j) \in \bar{\mathcal{X}}$:

$$\begin{aligned} u_{ij}^*(x) = \underset{u_{ij}(x)}{\arg\min} \int_0^R u_{ij}(x) \ln\left(\frac{u_{ij}(x)}{v_{ij}(x)}\right) \mathrm{d}x, & \\ \text{s.t.} \int_0^R \phi_{b_{ij}}(x) \mathrm{d}U_{ij}(x) = \beta_{b_{ij}}, \qquad \forall b_{ij} \in \mathcal{B}_{ij} & \\ \int_0^R u_{ij}(x) \mathrm{d}x = 1, & \\ u_{ij}(x) \geq 0. & \end{aligned} \tag{13}$$

The following theorem provides the expression for the optimal marginal utility density functions in GOPA-RUE.

Theorem 1 *Let $\boldsymbol{\lambda} \in \mathbb{R}^{B_{ij}}$ and $\lambda_0 \in \mathbb{R}$ denote the Euler-Lagrange operators corresponding to the MTP constraints and the normalization constraint for any $(i, j) \in \bar{\mathcal{X}}$, respectively. The optimal marginal utility density function $u_{ij}^*(x)$ for the lower-level problem of GOPA-RUE in Equation (13) is given by*

$$u_{ij}^*(x) = v_{ij}(x) e^{-1-\lambda_0 - \sum_{b_{ij} \in \mathcal{B}_{ij}} \lambda_{b_{ij}} \phi_{b_{ij}}(x)}, \tag{14}$$

which is a piecewise function with breakpoints at $r_{c_{ij}}$ for all $c_{ij} \in \mathcal{C}_{ij}$.

The following corollary shows that the utility entropy maximization without reference marginal utility structure is a special case of the relative utility entropy minimization in GOPA-RUE when the reference marginal utility density function is uniform.

Corollary 1 *Let* $\bar{v}(x)$ *denote the uniform marginal utility density function on* $(0, R]$. *For any* $(i, j) \in \bar{\mathcal{X}}$, *there exists*

$$u^*_{ij}(x) = \mathop{\arg\max}_{u_{ij}(x)\in\mathcal{P}_{ij}\cap\mathcal{U}} -\int_0^R u_{ij}(x)\ln\left(u_{ij}(x)\right)\mathrm{d}x = \bar{v}(x)e^{-1-\lambda_0-\sum_{b_{ij}\in\mathcal{B}_{ij}}\lambda_{b_{ij}}\phi_{b_{ij}}(x)} \tag{15}$$

where $\boldsymbol{\lambda} \in \mathbb{R}^{B_{ij}}$ *and* $\lambda_0 \in \mathbb{R}$ *are Euler-Lagrange operators.*

Although Theorem 1 characterize the optimal marginal utility density function, the Euler-Lagrange operators necessary for solving the lower-level problem of GOPA-RUE remain undetermined. Therefore, the primary task in the subsequent analysis is to derive the Euler-Lagrange operators by exploiting the structural properties inherent in GOPA-RUE.

Notice that $\sum_{b_{ij}\in\mathcal{B}_{ij}}\lambda_{b_{ij}}\phi_{b_{ij}}(x)$ is the aggregation of step function $\phi_{b_{ij}}(x)$ with the coefficient $\lambda_{b_{ij}}$ for $(i, j) \in \bar{\mathcal{X}}$, which ensures $e^{-1-\lambda_0-\sum_{b_{ij}\in\mathcal{B}_{ij}}\lambda_{b_{ij}}\phi_{b_{ij}}(x)}$ is a unique step function defined over each intervals given any set of Euler-Lagrange operators. This property motivates the following proposition for obtaining the optimal marginal utility density function of GOPA-RUE through a system of equations.

Proposition 2 *Let*

$$\Delta V_{c_{ij}} = \int_{r_{c_{ij}-1}}^{r_{c_{ij}}} v_{ij}(x)\mathrm{d}x,$$

$$g_{c_{ij}} = e^{-1-\lambda_0-\sum_{b_{ij}\in\mathcal{B}_{ij}}\lambda_{b_{ij}}\phi_{b_{ij}}(r_{c_{ij}})},$$

for all $c_{ij} \in \mathcal{C}_{ij}$ *and* $(i, j) \in \bar{\mathcal{X}}$, *and*

$$\bar{\boldsymbol{\phi}}_{b_{ij}} = \left(\mathbf{1}\left\{r_{b_{ij}} \in (r_1, +\infty)\right\}, \ldots, \mathbf{1}\left\{r_{b_{ij}} \in (r_{C_{ij}}, +\infty)\right\}\right)^{\mathrm{T}},$$

for all $b_{ij} \in \mathcal{B}_{ij}$ *and* $(i, j) \in \bar{\mathcal{X}}$. *Define*

$$\boldsymbol{\Delta V}_{ij} = \begin{bmatrix} \Delta V_1 & & \\ & \ddots & \\ & & \Delta V_{C_{ij}} \end{bmatrix},$$

$\boldsymbol{g}_{ij} = (g_1, \ldots, g_{C_{ij}})^{\mathrm{T}}$, $\boldsymbol{\beta}_{ij} = (\beta_1, \ldots, \beta_{B_{ij}}, 1)^{\mathrm{T}}$, *and* $\boldsymbol{\Psi}_{ij} = (\boldsymbol{\psi}_1, \ldots, \boldsymbol{\psi}_{B_{ij}}, \boldsymbol{e})^{\mathrm{T}}$, *where* $\boldsymbol{\psi}_{b_{ij}} = \bar{\boldsymbol{\phi}}_{b_{ij}} - \alpha_{b_{ij}}\bar{\boldsymbol{\phi}}_{b'_{ij}}$ *and* $\boldsymbol{e}$ *is a* C_{ij}*-dimensional vector of all ones for all* $(i, j) \in \bar{\mathcal{X}}$.

The optimal marginal utility density function $u^*_{ij}(x)$ *for the lower-level problem of GOPA-RUE is given by*

$$u^*_{ij}(x) = \sum_{c_{ij}\in\mathcal{C}_{ij}} g^*_{c_{ij}} v_{ij}(x)\mathbf{1}\left\{x \in (r_{c_{ij}-1}, r_{c_{ij}}]\right\}, \tag{16}$$

where $g^*_{c_{ij}}$ *is the solution of the following system of equations:*

$$\boldsymbol{\Psi}_{ij}\boldsymbol{\Delta V}_{ij}\boldsymbol{g}_{ij} = \boldsymbol{\beta}_{ij}. \tag{17}$$

It is important to clarify how the induced utilities depend on the reference function. When $\boldsymbol{\Psi}_{ij}$ and $\boldsymbol{\beta}_{ij}$ are fixed for any $(i, j) \in \bar{\mathcal{X}}$, the solution of the lower-level linear system depends on the reference only through the interval masses $\Delta V_{c_{ij}} = \int_{r_{c-1}}^{r_c} v_{ij}(x)\mathrm{d}x$. In contrast, the induced utilities $U_{ijr}^{*} = \int_{0}^{R-r+1} u_{ij}^{*}(x)\mathrm{d}x$ generally depend on truncated integrals of $v_{ij}(x)$ within intervals whenever $R - r + 1$ does not coincide with a partition point. Because the partition points constitute a subset of $\mathcal{R}$, U_{ijr}^{*} cannot, in general, be characterized solely by the interval masses $\Delta V_{c_{ij}}$ and may differ across reference functions sharing the same $\Delta V_{c_{ij}}$. In the special case where all partition points align with $\mathcal{R}$, however, the induced utilities reduce to sums of complete interval masses and are fully determined by $\Delta V_{c_{ij}}$.

The following lemma establishes that the matrix induced by the MTP elicitation strategy possesses full column rank, which guarantees the nonsingularity of the associated Gram matrix.

Lemma 1 *For any $(i, j) \in \bar{\mathcal{X}}$, let $\boldsymbol{A}_{ij} := \boldsymbol{\Psi}_{ij}\boldsymbol{\Delta V}_{ij}$ be defined as in Proposition 2. Under the MTP elicitation strategy specified in Section 4.2.2, $\boldsymbol{A}_{ij}$ has full column rank, i.e.,* $\operatorname{rank}(\boldsymbol{A}_{ij}) = C_{ij}$. *Consequently, $\boldsymbol{A}_{ij}^{\top}\boldsymbol{A}_{ij}$ is nonsingular.*

Although Proposition 2 characterizes the optimal marginal utility density of GOPA-RUE through a linear system, exact feasibility of this system cannot be guaranteed in practice. This limitation is unavoidable, as DMs' elicited preference judgments may contain inconsistencies or contradictions due to cognitive limitations or bounded rationality. Consequently, rather than enforcing exact satisfaction of the system, I determine $\boldsymbol{g}_{ij}$ as a best-fitting solution that balances data fidelity and robustness. In particular, regularization is introduced to stabilize the estimation against ill-conditioned or noisy preference information and to ensure a unique solution. Leveraging the full column rank property established in Lemma 1, I therefore adopt a regularized least-squares formulation, which admits a closed-form solution.

Proposition 3 *For any $(i, j) \in \bar{\mathcal{X}}$, let $\boldsymbol{A}_{ij} := \boldsymbol{\Psi}_{ij}\boldsymbol{\Delta V}_{ij}$ be defined as in Proposition 2. For any $\lambda > 0$, the unconstrained regularized least-squares problem:*

$$\min_{\boldsymbol{g}_{ij}} \ \frac{1}{2}\left\|\boldsymbol{A}_{ij}\boldsymbol{g}_{ij} - \boldsymbol{\beta}_{ij}\right\|_2^2 + \frac{\lambda}{2}\left\|\boldsymbol{g}_{ij}\right\|_2^2 \tag{18}$$

admits the unique closed-form solution:

$$\boldsymbol{g}_{ij}^{*} = \left(\boldsymbol{A}_{ij}^{\top}\boldsymbol{A}_{ij} + \lambda\boldsymbol{I}\right)^{-1}\boldsymbol{A}_{ij}^{\top}\boldsymbol{\beta}_{ij}. \tag{19}$$

The solution in Proposition 3 is computationally efficient and uniquely defined. I subsequently perform a post-solution feasibility check. If the resulting $\boldsymbol{g}_{ij}^{\star}$ satisfies the nonnegativity requirement, it is adopted as the final estimate. Otherwise, I enforce the nonnegativity constraint explicitly by solving the following nonnegative regularized least-squares problem:

$$\min_{\boldsymbol{g}_{ij}\geq 0} \ \frac{1}{2}\left\|\boldsymbol{A}_{ij}\boldsymbol{g}_{ij} - \boldsymbol{\beta}_{ij}\right\|_2^2 + \frac{\lambda}{2}\left\|\boldsymbol{g}_{ij}\right\|_2^2. \tag{20}$$

When the elicited MTP constraints are internally inconsistent, the regularized (nonnegative) least-squares formulations should be understood as relaxations of the exact linear system characterized in Proposition 2. In this case, the recovered marginal utility density does not represent an exact preference-consistent structure, but rather a best-fitting approximation that balances conflicting judgments while preserving stability and nonnegativity. This relaxation does not affect the validity of the upper-level optimization. Accordingly, the resulting decision weights are optimal with respect to the approximated preference model, ensuring robustness of GOPA-RUE under noisy or contradictory preference information.

The following corollary establishes that the optimal marginal utility density function of GOPA-RUE shares the same risk preference as the reference utility density function within each interval defined by the breakpoints.

Corollary 2 *For any $(i, j) \in \bar{\mathcal{X}}$, by Arrow-Pratt's definition of the risk preference function, the local risk preference $\eta_{ij}(x)$ of the optimal utility density function $u_{ij}^*(x)$ of GOPA-RUE in Equation (13) is given by*

$$\eta_{ij}(x) = \sum_{c_{ij} \in \mathcal{C}_{ij}} \left(-\frac{\mathrm{d}}{\mathrm{d}x} \ln(v_{ij}(x)) \right) \mathbf{1}\left\{ x \in (r_{c_{ij}-1}, r_{c_{ij}}] \right\}, \quad \forall x \in (0, R]. \tag{21}$$

Corollary 2 indicates that the risk preference of the optimal marginal utility density function of GOPA-RUE can be controlled by choosing appropriate reference utility functions. Therefore, in minimizing relative utility entropy, partial preference constraints primarily determine the utility function, while the reference utility primarily adjusts within the defined intervals. In the absence of a reference utility structure, Corollary 2 suggests that utility entropy maximization can be used to derive utility with risk-neutral preferences. In addition, the results from the lower-level estimation of GOPA-RUE in the continuous setting can be naturally extended to the discrete case, where the reference utility structure can be represented through rank based surrogate weights.

4.3.2 Upper-level optimization for decision weights

After determining the optimal marginal utility functions for all $(i, j) \in \bar{\mathcal{X}}$ from the lower-level preference learning problem, I proceed to the upper-level optimization of GOPA-RUE, which aims to determine the decision weights:

$$\begin{aligned}
&\max_{\bar{\boldsymbol{w}}, z} \; z, \\
&\text{s.t. } RU_{ijr}^* z \leq t_i s_{ij} \bar{w}_{ijr}, && \forall (i, j, r) \in \mathcal{Y}, \\
&\quad U_{ijr}^* = \int_0^{R-r+1} u_{ij}^*(x) \mathrm{d}x, && \forall (i, j, r) \in \mathcal{Y}, \\
&\quad \sum_{i \in \mathcal{I}} \sum_{k \in \mathcal{K}} \sum_{r \in \mathcal{R}} \bar{w}_{ijr} = 1, \\
&\quad \bar{w}_{ijr} \geq 0, && \forall (i, j, r) \in \mathcal{Y}.
\end{aligned} \tag{22}$$

The following theorem presents the closed-form solution of the upper-level problem of GOPA-RUE.

Theorem 2 *The closed-form solution of GOPA in Equation (22) is given by*

$$z^* = \left(\sum_{i \in \mathcal{I}} \sum_{j \in \mathcal{J}} \sum_{r \in \mathcal{R}} \frac{RU_{ijr}^*}{t_i s_{ij}} \right)^{-1}, \tag{23}$$

and

$$\bar{w}_{ijr}^* = \frac{RU_{ijr}^* z^*}{t_i s_{ij}}, \quad \forall (i, j, r) \in \mathcal{Y}, \tag{24}$$

Especially, the closed-form solution of OPA-II can be obtained by replacing U_{ijr}^* with U_r^{ROC}.

Theorem 2 shows that the upper-level solution follows a normalized proportional allocation rule, where weights are assigned according to marginal utility adjusted by structural scaling factors. The term z^* acts as a normalization constant ensuring feasibility. The solution reflects global competition across alternatives and allows transparent comparative statics.

Importantly, the closed-form expression eliminates the need to solve the original upper-level optimization problem numerically, enabling direct computation from given parameters and substantially improving computational efficiency. In addition, the closed-form solution provides a general lower bound reference for various weight elicitation methods, extending beyond GOPA. In this study, the subjective preference-based weight elicitation approach emphasizes the unknown weight benchmark (lower bound), setting it apart from other weight elicitation problems, such as portfolio decision-making. In portfolio decision-making, a benchmark return, like the performance of an existing portfolio or market index, serves as a reference. Likewise, the closed-form solution in Theorem 2 offers a comparable benchmark for the broader problem of weight elicitation based on subjective preferences.

The following corollary demonstrates that the optimal GOPA-RUE weights can be decomposed into the components independently determined by the ranking indices of experts, attributes, and alternatives.

Corollary 3 *Given*

$$\bar{z}^* = \left(\sum_{i \in \mathcal{I}} \sum_{j \in \mathcal{J}} \frac{R}{t_i s_{ij}} \right)^{-1},$$

and the rank reciprocal weight for an object ranked l, i.e., $w_l^{RR} = (\sum_{h=l}^{L} \frac{1}{h})/L$ for all $l \in [L]$, the optimal GOPA-RUE weights are equivalent to

$$\bar{w}_{ijr}^* = w_{t_i}^{RR} w_{s_{ij}}^{RR} w_{ijr}^{MRU}, \quad \forall (i, j, r) \in \mathcal{Y}, \tag{25}$$

where $w_{ijr}^{MRU} = \frac{z^*}{\bar{z}^*} U_{ijr}^*$ satisfying

(1) [Monotonicity] $w_{ijr}^{MRU} > w_{ijr+1}^{MRU}$ for all $r = 1, \dots, R-1$ and $(i, j) \in \bar{\mathcal{X}}$;
(2) [Normalization] $\sum_{i \in \mathcal{I}} \sum_{j \in \mathcal{J}} \sum_{r \in \mathcal{R}} w_{ijr}^{MRU} = 1$.

Especially, the decomposability of the optimal weights of OPA-II can be obtained by replacing w_{ijr}^{MRU} with w_r^{ROC}.

Corollary 3 not only demonstrates the decomposability of the GOPA-RUE solution but also provides a normalization factor for utility derived from the minimum relative utility entropy across all $(i, j) \in \bar{\mathcal{X}}$. This forms the theoretical foundation for a more flexible GOPA-RUE prescription, where expert weights, attribute weights across different experts, and alternative utilities can be customized. It also explains the rationale for multiplying the weight disparities of consecutively ranked alternatives by the rankings of experts, attributes, and alternatives in OPA-I: this results in a composite weight comprising RR weights for the ranked experts, RR weights for the attributes, and ROC weights for the alternatives. Additionally, Corollary 3 implies that the optimal GOPA-RUE weights can be derived by solving the linear programming problem for each attribute under each expert, followed by aggregating the results based on expert and attribute weights. Thus, it mitigates divergent group consensus encountered in MADM methods such as AHP and BWM.

The following algorithm summarizes the computational procedure for GOPA-RUE. For each $(i, j) \in \bar{\mathcal{X}}$, constructing $\boldsymbol{A}_{ij} = \boldsymbol{\Psi}_{ij} \boldsymbol{\Delta} V_{ij}$ requires $\mathcal{O}(B_{ij} C_{ij})$ operations. Solving the unconstrained regularized least-squares problem entails forming $\boldsymbol{A}_{ij}^\top \boldsymbol{A}_{ij}$ and solving a $C_{ij} \times C_{ij}$ linear system, which requires $\mathcal{O}(C_{ij}^3)$ time. The subsequent nonnegativity check incurs linear time in C_{ij}; when violated, the nonnegative regularized least-squares problem can be solved in polynomial time and typically exhibits $\mathcal{O}(C_{ij}^3)$ worst-case complexity under standard active-set or projected-gradient methods. Constructing the marginal utility density and computing the induced utilities $\{U^*_{ijr}\}_{r\in\mathcal{R}}$ require $\mathcal{O}(C_{ij}+|\mathcal{R}|)$ operations. Aggregating over all $(i, j) \in \bar{\mathcal{X}}$, the total computational cost of the lower-level preference learning stage is $\mathcal{O}\Big(\sum_{(i,j)\in\bar{\mathcal{X}}} C^3_{ij}\Big)$, which dominates the remaining steps. The computation of z^*, $\{\bar{w}^*_{ijr}\}$, and the global weights involves only summations over index sets and incurs $\mathcal{O}(|\mathcal{I}||\mathcal{J}||\mathcal{R}| + |\mathcal{I}||\mathcal{J}||\mathcal{K}|)$ time. Overall, Algorithm 1 runs in polynomial time and remains computationally tractable for moderate numbers of breakpoints and decision dimensions.

Algorithm 1 Algorithm for GOPA-RUE

Input: R, $\{t_i\}$, $\{s_{ij}\}$, $\{v_{ij}(x)\}$, $\{\boldsymbol{\Psi}_{ij}\}$, $\{\boldsymbol{\Delta V}_{ij}\}$, $\{\boldsymbol{\beta}_{ij}\}$, and λ for all $(i, j) \in \bar{\mathcal{X}}$.
for $(i, j) \in \bar{\mathcal{X}}$ **do**
  Construct $\boldsymbol{A}_{ij} = \boldsymbol{\Psi}_{ij}\boldsymbol{\Delta V}_{ij}$.
  Compute the unconstrained regularized least-squares solution:

$$\boldsymbol{g}^{\star}_{ij} = \left(\boldsymbol{A}^{\top}_{ij}\boldsymbol{A}_{ij} + \lambda\boldsymbol{I}\right)^{-1}\boldsymbol{A}^{\top}_{ij}\boldsymbol{\beta}_{ij}.$$

  if $\boldsymbol{g}^{\star}_{ij} \geq 0$ **then**
    Set $\boldsymbol{g}^*_{ij} = \boldsymbol{g}^{\star}_{ij}$.
  else
    Solve the nonnegative regularized least-squares problem:

$$\boldsymbol{g}^*_{ij} = \arg\min_{\boldsymbol{g}_{ij}\geq 0} \frac{1}{2}\|\boldsymbol{A}_{ij}\boldsymbol{g}_{ij} - \boldsymbol{\beta}_{ij}\|^2_2 + \frac{\lambda}{2}\|\boldsymbol{g}_{ij}\|^2_2.$$

  end if
  Construct the marginal utility density $u^*_{ij}(x) = \sum_{c_{ij}\in\mathcal{C}_{ij}} g^*_{c_{ij}} v_{ij}(x)\mathbf{1}\{x \in (r_{c_{ij}-1}, r_{c_{ij}}]\}$.
  for $r \in \mathcal{R}$ **do**
    Compute the induced utility $U^*_{ijr} = \int_0^{R-r+1} u^*_{ij}(x)\mathrm{d}x$.
  end for
end for
Compute the optimal weight disparity scalar $z^* = \left(\sum_{i\in\mathcal{I}}\sum_{j\in\mathcal{J}}\sum_{r\in\mathcal{R}} \frac{RU^*_{ijr}}{t_i s_{ij}}\right)^{-1}$.
for $(i, j, r) \in \mathcal{Y}$ **do**
  Compute the weight of the ranked alternatives under experts and attributes $\bar{w}^*_{ijr} = \frac{RU^*_{ijr}z^*}{t_i s_{ij}}$.
  Map $\bar{w}^*_{ijr}$ to w^*_{ijk} based on alternative rankings.
end for
Calculate global weights:

$$W^{\mathcal{I}}_i = \sum_{j\in\mathcal{J}}\sum_{k\in\mathcal{K}} w^*_{ijk},\ \forall i \in \mathcal{I},\quad W^{\mathcal{J}}_j = \sum_{i\in\mathcal{I}}\sum_{k\in\mathcal{K}} w^*_{ijk},\ \forall j \in \mathcal{J},\quad W^{\mathcal{K}}_k = \sum_{i\in\mathcal{I}}\sum_{j\in\mathcal{J}} w^*_{ijk},\ \forall k \in \mathcal{K}.$$

Output: $\{U^*_{ijr}\}$, $\{\bar{w}^*_{ijr}\}$, $\{w^*_{ijk}\}$, $\{W^{\mathcal{I}}_i\}$, $\{W^{\mathcal{J}}_j\}$, $\{W^{\mathcal{K}}_k\}$, and z^*.

4.4 Sensitivity analysis

This section conducts the sensitivity analysis of GOPA-RUE, including the perturbations of constraints, ranking parameters, and alternative utilities, using the respective dual reformulation.

Consider the perturbation problem of GOPA-RUE for constraint perturbations:

$$\begin{aligned}
&\max_{z,\bar{\boldsymbol{w}}} z, \\
&\text{s.t. } t_i s_{ij} \bar{w}_{ijr} - RU^*_{ijr} z \geq \varepsilon_{ijr}, \qquad \forall (i,j,r) \in \mathcal{Y}, \\
&\quad 1 - \sum_{i\in\mathcal{I}} \sum_{j\in\mathcal{J}} \sum_{r\in\mathcal{R}} \bar{w}_{ijr} = \epsilon, \\
&\quad \bar{w}_{ijr} \geq 0, \qquad \forall (i,j,r) \in \mathcal{Y},
\end{aligned} \tag{26}$$

which is assumed to be feasible. The perturbation parameters can be both positive and negative, leading to changes in the right-hand side of the normalization constraint by ϵ, as well as tightening or relaxing the inequalities of weight disparity constraints by ε_{ijr} for all $(i, j, r) \in \mathcal{Y}$. The following theorem presents the sensitivity analysis results for the constraint perturbation problem.

Theorem 3 *Let $(z^*(\boldsymbol{\varepsilon}, \epsilon), \bar{\boldsymbol{w}}^*(\boldsymbol{\varepsilon}, \epsilon))$ denote the optimal solution of the constraint perturbation problem of GOPA-RUE in Equation (26). Then,*

$$z^*(\boldsymbol{\varepsilon}, \epsilon) \leq \left(1 - \epsilon - \sum_{i\in\mathcal{I}} \sum_{j\in\mathcal{J}} \sum_{r\in\mathcal{R}} \frac{\varepsilon_{ijr}}{t_i s_{ij}}\right) z^*, \tag{27}$$

and

$$\bar{w}^*_{ijr}(\boldsymbol{\varepsilon}, \epsilon) = \frac{RU^*_{ijr} z^*(\boldsymbol{\varepsilon}, \epsilon)}{t_i s_{ij}}, \quad \forall (i,j,r) \in \mathcal{Y}. \tag{28}$$

where z^* is given by Equation (23).

Theorem 3 shows that reducing the normalization scale (equality constraint) or tightening the weight disparity constraints (inequality constraints) results in a smaller optimal weight disparity scalar, which follows a linear relationship. The sensitivity of the optimal weights is determined by the weight disparity scalar.

I then analyze the sensitivity of GOPA-RUE with respect to the ranking parameters of experts and attributes, as well as the utilities for ranked alternatives. Consider the perturbation problem of GOPA-RUE for ranking parameter:

$$\begin{aligned}
&\max_{z,\bar{\boldsymbol{w}}} z, \\
&\text{s.t. } R(U^*_{ijr} + \delta_{ijr}) z \leq (t_i s_{ij} + \sigma_{ij}) \bar{w}_{ijr}, \qquad \forall (i,j,r) \in \mathcal{Y}, \\
&\quad \sum_{i\in\mathcal{I}} \sum_{j\in\mathcal{J}} \sum_{r\in\mathcal{R}} \bar{w}_{ijr} = 1, \\
&\quad \bar{w}_{ijr} \geq 0, \qquad \forall (i,j,r) \in \mathcal{Y},
\end{aligned} \tag{29}$$

which is assumed to be feasible.

Corollary 4 *Let $z^*(\boldsymbol{\delta}, \boldsymbol{\sigma})$ and $\bar{\boldsymbol{w}}^*(\boldsymbol{\delta}, \boldsymbol{\sigma})$ denote the optimal solution of the ranking perturbation problem of GOPA-RUE in Equation (29). Then,*

$$z^*(\boldsymbol{\delta}, \boldsymbol{\sigma}) = \left(\sum_{i\in\mathcal{I}} \sum_{j\in\mathcal{J}} \sum_{r\in\mathcal{R}} \frac{R(U^*_{ijr} + \delta_{ijr})}{t_i s_{ij} + \sigma_{ij}}\right)^{-1}, \tag{30}$$

and

$$\bar{\boldsymbol{w}}^*_{ijr}(\boldsymbol{\delta},\boldsymbol{\sigma}) = \frac{R(U^*_{ijr}+\delta_{ijr})z^*(\boldsymbol{\delta},\boldsymbol{\sigma})}{t_i s_{ij}+\sigma_{ij}}, \quad \forall(i,j,r)\in\mathcal{Y}. \tag{31}$$

Corollary 4 illustrates that the sensitivity of the optimal weight disparity scalar is linearly related to the utility perturbation and inversely proportional to the ranking parameter perturbation. The optimal weights mirror the optimal weight disparity scalar and are linearly related to its perturbation.

Equations (27) and (30) further allow the identification of robustness regions for the optimal solution. In particular, as long as

$$1-\epsilon-\sum_{i\in\mathcal{I}}\sum_{j\in\mathcal{J}}\sum_{r\in\mathcal{R}}\frac{\varepsilon_{ijr}}{t_i s_{ij}}>0,$$

the perturbed problem in (26) remains well defined and the optimal weight disparity scalar $z^*(\boldsymbol{\varepsilon},\epsilon)$ is bounded. Similarly, bounded perturbations $(\boldsymbol{\delta},\boldsymbol{\sigma})$ yield explicit bounds on $z^*(\boldsymbol{\delta},\boldsymbol{\sigma})$ through (30), thereby providing a transparent robustness characterization of GOPA-RUE with respect to ranking and utility perturbations.

5 Numerical Experiment

5.1 Problem setup

This study selects the improvisational emergency supplier selection (IESS) during the 7.20 mega-rainstorm disaster in Zhengzhou, China, as a case study to demonstrate GOPA-RUE (Peng and Zhang, 2022). Unlike regular emergency supplier selection, IESS has distinct characteristics. Regular emergency supplier selection typically occurs during the emergency preparedness phase; however, the complexity and unpredictability of disasters may render pre-selected suppliers inadequate for disaster response (Wang et al., 2022). In such situations, IESS becomes essential. IESS requires rapid decision-making under tight time constraints and high uncertainty, making it challenging to obtain high-quality data and often necessitating reliance on partial preference information. Additionally, due to time pressure and information uncertainty, DMs' risk preferences significantly influence decision-making. Overall, the reason for selecting IESS to illustrate the applicability and effectiveness of GOPA-RUE is that it aligns with the decision analysis framework of GOPA-RUE, and the urgency and complexity of decision-making in this scenario provide an ideal testing platform.

There are 10 emergency suppliers (labeled A1 to A10) available for selection within the disaster area, each with distinct characteristics. Some emphasize stable supply chains and prompt response capabilities despite higher costs, while others utilize strategic geographic positioning and efficient transport connections to expedite flood relief efforts during crises. Attributes selected for IESS include response speed (C1), delivery reliability (C2), geographic coverage (C3), operational sustainability (C4), collaborative experience and credibility (C5), and supply cost (C6) (Wang et al., 2025). Five DMs (labeled E1 to E5) from various departments act as stakeholders for IESS, prioritized based on their decision-making authority as E5>E2>E1>E3>E4. These DMs provides their risk preference to each attribute, rankings of attributes and alternatives, and sufficiently determined partial preference information, as detailed in Online Supplemental Material.

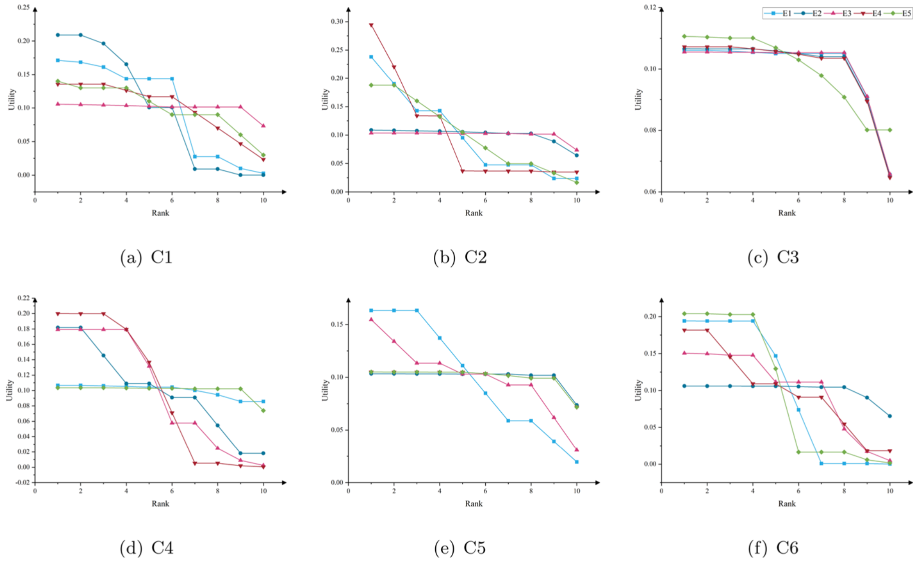

(a) C1 (b) C2 (c) C3

(d) C4 (e) C5 (f) C6

Fig. 2 Calculation results of utilities

5.2 Experiment result

Figure 2 reports the optimal utilities of ranked alternatives across attributes based on experts' partial preference information. The results reveal substantial heterogeneity in utility gaps across both attributes and experts, highlighting the importance of explicitly incorporating partial preference information in utility elicitation. For instance, under C2, the utility for E4 declines from 0.295 at rank $r = 1$ to 0.220 at $r = 2$ and further to 0.134 at $r = 3$, whereas under C3, the E3's utility remains close to 0.1055 for $r = 1$ and $r = 4$ before decreasing at lower ranks. Utility decay also varies markedly by attribute: under C6, E5's utility drops sharply from 0.204 at $r = 1$ to 0.016 at $r = 6$ and 0.002 at $r = 10$, indicating a strong emphasis on top-ranked alternatives, while attributes such as C3 exhibit a more gradual decline, from approximately 0.106 at $r = 1$ to about 0.066 at $r = 10$. Apparent similarities across adjacent ranks (e.g., values around 0.105-0.107 under C3) are due to numerical rounding rather than true flat segments in the underlying utilities.

Figure 3 reports the resulting weights and rankings of experts, attributes, and alternatives. The expert weights exhibit a clear hierarchical structure: E5 is the most influential expert with a weight of 0.438, followed by E2 at 0.219. The remaining experts, E1, E3, and E4, receive weights of 0.146, 0.110, and 0.088, respectively, reflecting the diminishing marginal effects implied by the RR weighting scheme. In terms of attributes, response speed (C1) is identified as the most critical criterion with a weight of 0.271, indicating its central role in emergency supplier selection. Collaborative experience and credibility (C5) ranks second at 0.226, underscoring the importance of coordination and trust in humanitarian operations. Delivery reliability (C2) and geographic coverage (C3) receive moderate emphasis, with weights of 0.166 and 0.148, respectively. By contrast, supply cost (C6) and operational sustainability (C4) are assigned relatively lower weights of 0.114 and 0.075. Notably, despite the increasing global emphasis on sustainability-oriented practices, stakeholders in this case study perceive operational sustainability as less critical in urgent emergency contexts, where

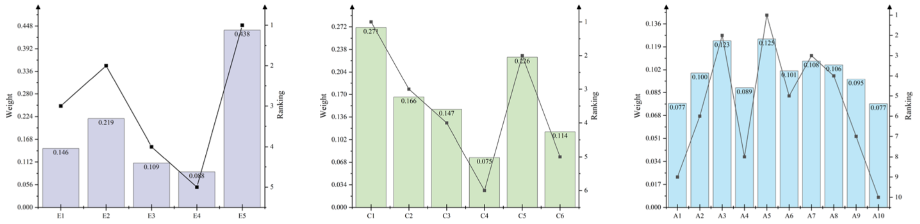

(a) Expert (b) Attribute (c) Alternative

Fig. 3 Calculation results of weights

responsiveness and coordination dominate decision priorities. Regarding alternative evaluation, A5 emerges as the top-ranked option with the highest weight of 0.125, closely followed by A3 at 0.123 and A7 at 0.109, indicating strong competition among the leading suppliers. A8 ranks fourth with a weight of 0.106, while the remaining alternatives exhibit noticeably lower weights, reflecting weaker overall performance across the evaluated attributes. Collectively, these results suggest that A5 represents the most preferred emergency supplier, with A3 and A7 serving as viable secondary choices, thereby providing a clear and interpretable ranking outcome for managerial decision making.

5.3 Ablation analysis

This section reports an ablation analysis to isolate the contributions of key design components in GOPA-RUE and to examine the sensitivity of the resulting alternative rankings. Beyond quantifying the performance loss from removing or simplifying individual components, the analysis clarifies the mechanisms through which GOPA-RUE operates by disentangling the roles of MTP information and the reference function shaping utility. Six GOPA-RUE variants are constructed by activating or deactivating MTPs and combining them with three reference functions, Uniform (non-informative baseline), S-shape, and HARA, yielding 2×3 configurations. The original OPA model is included as a purely rank-based benchmark without utility reconstruction. For each configuration, aggregated alternative weights and rankings are computed, and a Spearman rank-correlation matrix is reported to evaluate robustness and structural similarity across ablation settings. Results are presented in Fig. 4.

Figure 4(a) reports alternative weights under the six GOPA-RUE variants and the OPA-ROC benchmark. Overall patterns are stable, yet distinct structural effects arise from MTPs and the reference function. Imposing MTP constraints (MTP+Uniform and MTP+S-shape) produces a more polarized distribution, concentrating weight on leading alternatives, particularly A5 (0.138 and 0.141), while A10 remains last in all cases. This polarization aligns with the theoretical role of MTPs in the lower-level entropy minimization problem: by embedding local structural information on adjacent ranked utilities, they amplify disparities implied by ordinal dominance. Removing MTPs (Uniform and S-shape) yields smoother and more evenly distributed weights, as utilities are then governed solely by the reference function and normalization. The reference function exerts the strongest influence under HARA. Unlike Uniform and S-shape, which mainly adjust marginal curvature around middle ranks, HARA reshapes the global curvature of the utility density, reallocating mass across both top- and mid-ranked alternatives. Consequently, A1, A4, and A6 gain relative weight, and the overall profile becomes flatter, even with MTPs. These systematic differences reflect structural

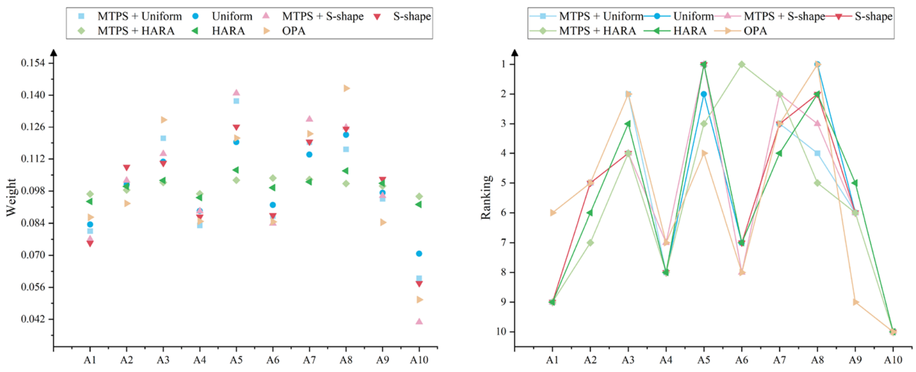

(a) Alternative weight

(b) Alternative ranking

Fig. 4 Results of ablation analysis

trade-offs between entropy regularization and MTP constraints rather than numerical noise. In contrast, OPA-ROC assigns substantial weight to A8 (0.143) and A3 (0.129), illustrating the concentration induced by ROC-based rank-to-weight transformation and confirming that GOPA-RUE's utility reconstruction fundamentally alters the mapping from ordinal inputs to cardinal weights.

Figure 4(b) indicates that overall rankings are broadly robust across settings, yet the top-ranked alternative is highly sensitive to the interaction between MTPs and the reference function. Under MTP+Uniform and MTP+S-shape, A5 consistently ranks first, with A7 and A8 remaining within the top four. MTPs thus stabilize leading positions by amplifying dominance relations embedded in local moment information and by enforcing consistent marginal utility gaps between adjacent ranks, thereby counteracting entropy-induced smoothing. Without MTPs, the top position becomes reference-dependent. The Uniform reference-only case selects A8 as rank 1, whereas the S-shape reference-only case retains A5 at rank 1 but places A8 at rank 2. Hence, global curvature assumptions alone can alter the argmax even when the remaining order changes marginally. The largest shift occurs under MTP+HARA, where A6 rises to rank 1 and A5 drops to rank 3. This reflects a nonlinear interaction between HARA curvature and moment conditions: reshaping marginal utility decay across rank intervals sufficiently modifies cumulative utility gaps to change the top choice. The OPA-ROC benchmark selects A8 as rank 1 and demotes A9 to rank 9, resembling the reference-only cases and confirming that OPA is purely rank-driven. By contrast, GOPA-RUE integrates entropy regularization with preference constraints, which can materially reshape implied dominance relations under identical ordinal inputs.

The Spearman rank-correlation matrix in Fig. 5 provides a structural assessment of robustness. Correlations within the Uniform and S-shape families are uniformly high ($\rho \approx$ 0.94-0.99), including strong agreement between constraint-enabled and constraint-disabled variants (e.g., Uniform vs. S-shape reference-only, $\rho = 0.988$). When the reference function does not substantially distort marginal curvature, rankings remain structurally stable and MTPs primarily refine rather than overturn the order. In such cases, entropy regularization and the ordinal structure already imply similar utility configurations, and activating constraints mainly sharpens local disparities without altering global geometry. By contrast, correlations involving MTP+HARA are markedly lower, with particularly weak association with OPA ($\rho = 0.430$). This indicates a substantive structural shift: the HARA reference,

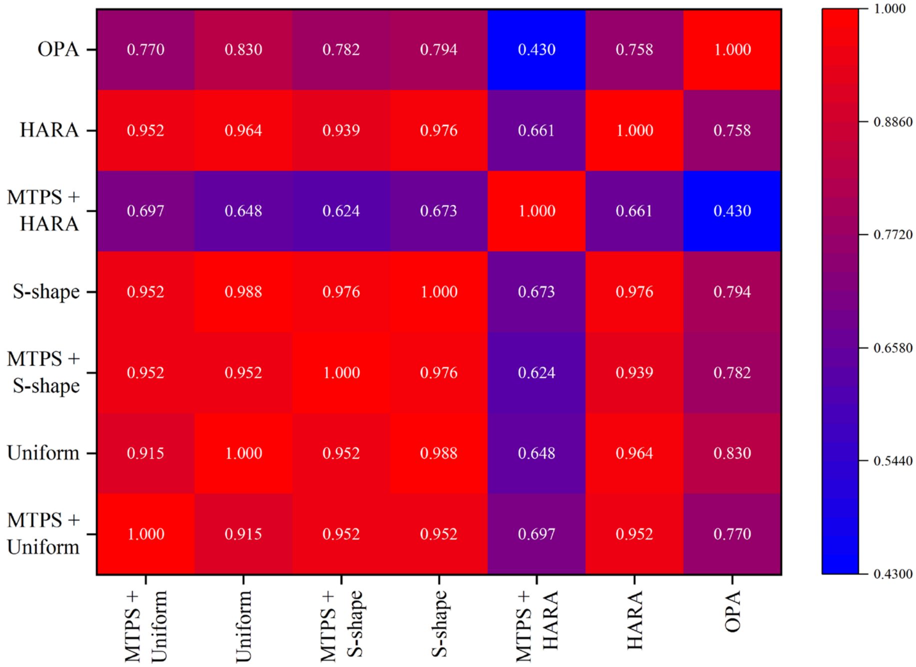

Fig. 5 Spearman rank-correlation

combined with MTPs, generates a qualitatively distinct utility landscape that materially alters ranking structure. OPA exhibits only moderate agreement with most GOPA-RUE variants, suggesting that ROC-based transformation captures part of the ordinal pattern but lacks the flexibility of entropy-based utility reconstruction. Overall, GOPA-RUE is robust under mild reference specifications (Uniform and S-shape), whereas nonlinear curvature adjustments can induce systematic reordering.

5.4 Sensitivity analysis

This section presents a sensitivity analysis covering preference parameter perturbation and ranking parameter perturbation.

5.4.1 Preference parameter perturbation

The preference parameter perturbation analysis evaluates the robustness of GOPA-RUE's utility estimates and alternative rankings to variations in partial preference information, focusing on the ratio-scale parameter α and absolute-difference parameter β in the moment-type preference set. Specifically, $\pm 10\%$ random perturbations are imposed on α and β for all expert-attribute pairs, generating 200 independent trials under a fixed random seed to ensure reproducibility. For each trial, the perturbed parameters redefine the constraint set, the lower-level regularized least-squares problem is solved to estimate utilities, and the upper-level decision weights are computed, with nonnegativity constraints imposed to guarantee feasible

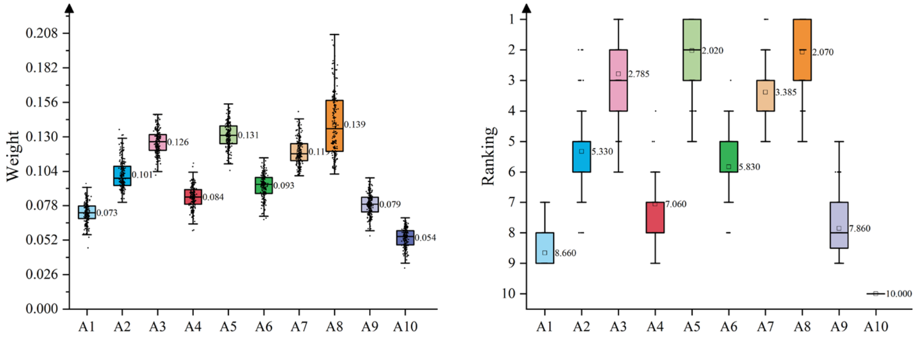

(a) Alternative weight (b) Alternative ranking

Fig. 6 Results of preference parameter perturbation

utility densities. The resulting weights and rankings are then compared with the baseline (unperturbed) outcomes. Results are presented in Fig. 6.

Figure 6(a) reports the distribution of alternative weights across 200 random perturbations of the preference parameters, with α and β varied within $\pm 10\%$. Mean weights closely align with the baseline, and 95% confidence intervals are narrow for most alternatives, indicating strong robustness to moderate fluctuations in preference intensity and difference levels. Top-ranked alternatives (mean weights $\approx$ 0.126-0.139) exhibit small standard deviations (about 0.009), suggesting structural stability under mild perturbations of moment-type constraints. One alternative with mean weight 0.139 shows a higher standard deviation (0.024), reflecting greater sensitivity near competitive boundaries among leading options. In such cases, small changes in α and β amplify marginal utility adjustments and increase dispersion. Mechanistically, α rescales utilities across ranked segments, whereas β shifts local moment constraints; both affect the estimated utility density $u_{ij}(x)$ in the lower-level entropy minimization. Nonetheless, normalization in both aggregation stages and averaging across experts and attributes absorb most local distortions, preventing substantial global deviations.

Figure 6(b) reports ranking statistics, further confirming structural robustness. For most alternatives, mean ranks remain close to baseline positions, with standard deviations typically between 0.6 and 1.2, indicating limited positional shifts. The worst alternative consistently ranks 10th across all trials (zero variance), showing that clearly dominated options are unaffected by local parameter changes. Leading alternatives with mean ranks near 2 also display narrow confidence intervals, confirming stable dominance relations. Greater dispersion appears among middle-ranked alternatives (mean ranks around 5-7), whose intervals span adjacent positions. This pattern is consistent with the GOPA-RUE mechanism: perturbations in α and β adjust the slope and curvature of the reconstructed marginal utility, slightly altering marginal gains among closely competing options. When weight differences are small, minor parameter changes can induce local reordering. However, the absence of large-scale rank reversals indicates that the global ordinal structure imposed by ranking parameters and normalized aggregation governs the outcome. Overall, Fig. 6 demonstrates that GOPA-RUE is locally responsive yet globally robust: perturbations affect fine discrimination among neighboring alternatives without disrupting the overall ranking structure.

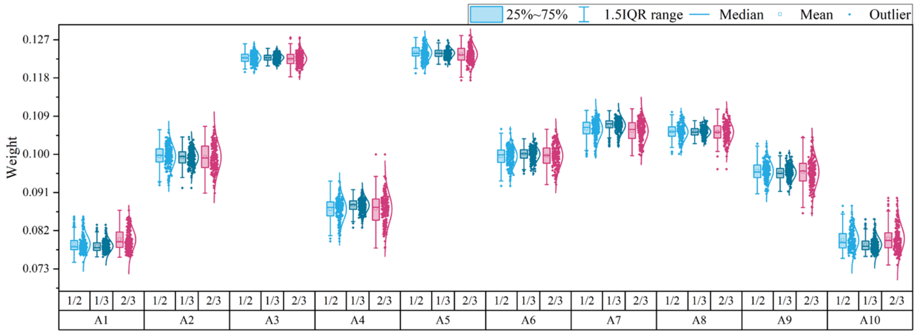

(a) Alternative weight

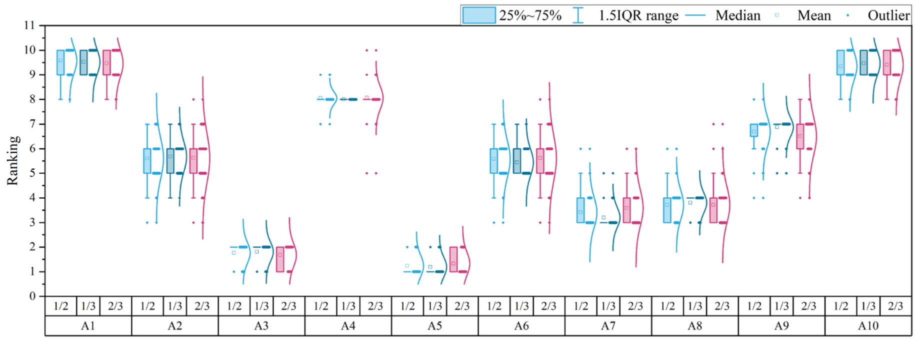

(b) Alternative ranking

Fig. 7 Results of ranking parameter perturbation

5.4.2 Ranking parameter perturbation

This section evaluates the robustness of GOPA-RUE to noise in experts' ranking parameters, which may arise from limited attention, ambiguity among closely ranked alternatives, or intra-expert inconsistency. To introduce controlled perturbations, each reported rank is modeled as the mean of a Gaussian distribution, and a perturbed continuous rank is drawn as $\tilde{r}_{ijk} \sim \mathcal{N}(r_{ijk}, \sigma^2)$ and truncated to $[1, R]$. Three noise levels are considered, $\sigma \in 1/3, 1/2, 2/3$, representing increasing perturbation intensity. By the empirical rule, 99.7% of mass lies within three standard deviations, implying that sampled ranks fall within approximately ± 1, ± 1.5, and ± 2 positions of the original rank with overwhelming probability, respectively. The perturbation is propagated to decision weights without re-solving the lower-level preference learning problem. Baseline reconstructed utilities, and thus $\bar{w}_{ijr}$ across rank positions, are held fixed, and perturbed alternative weights are obtained via linear interpolation. This design isolates the effect of ranking noise in the upper-level mapping, avoids confounding from re-estimated utilities, and captures realistic local rank swaps while preserving the ordinal structure of elicited inputs. Results are presented in Fig. 7.

Figure 7(a) presents the distribution of aggregated alternative weights under three levels of ranking noise, $\sigma \in \{1/3, 1/2, 2/3\}$. Mean weights remain highly stable across perturbations. The leading alternatives, A3 and A5, consistently exhibit mean weights of approximately

0.123-0.124, with standard deviations no greater than 0.002. Even at $\sigma = 2/3$, the 95% confidence intervals are extremely narrow; for A3, the mean is 0.123 with a standard deviation of 0.002. Most alternatives display standard deviations below 0.003. Although dispersion increases modestly with σ (e.g., for A4, from 0.002 at $\sigma = 1/3$ to 0.004 at $\sigma = 2/3$), overall variation remains limited. This stability arises because ranking noise affects only the upper-level interpolation from ranks to weights over the fixed $\bar{w}_{ijr}$ grid, while lower-level utility reconstruction and normalization remain unchanged. Since $\bar{w}_{ijr}$ varies smoothly across adjacent ranks and Gaussian perturbations induce primarily local shifts (typically within $\pm$1-2 positions), weight adjustments are small and further attenuated through aggregation across experts and attributes. Fig. 7(a) thus indicates strong numerical stability under moderate ranking noise.

Figure 7(b) reports ranking statistics, further confirming structural robustness. A3 and A5 consistently occupy the top two positions across all noise levels. At $\sigma = 1/3$, their mean ranks are 1.810 and 1.190, respectively, with standard deviations of 0.393; even at $\sigma = 2/3$, their mean ranks remain close to 1.675 and 1.325, and realized positions vary only between ranks 1 and 2. A4 is fully stable at $\sigma = 1/3$ (mean rank 8.000, standard deviation 0), indicating clear separation. As σ increases, variability becomes more pronounced among middle-ranked alternatives. For instance, A2's rank standard deviation rises from 0.617 to 1.015, and its range expands from [4, 7] to [3, 8]; similar patterns hold for A6, A7, and A8. This is consistent with the perturbation mechanism: alternatives with similar baseline weights are more sensitive to small interpolated changes, leading to occasional local swaps, whereas those separated by larger weight gaps exhibit strong persistence. Overall, ranking noise induces primarily local reordering among adjacent middle alternatives while preserving the global dominance structure. These results confirm that reconstructed utilities and normalized aggregation govern outcomes in GOPA-RUE, and moderate ordinal noise yields limited positional variation.

6 Concluding remarks

This study reexamines OPA from a structural perspective and establishes its equivalence to a ROC-weight formulation, thereby clarifying the theoretical foundation of its rank-to-weight transformation and decomposability. Building on this result, I propose GOPA, an estimate-then-optimize bilevel framework that replaces fixed ROC utilities with endogenously reconstructed marginal utilities derived from partial preference information. By introducing minimum relative utility entropy as the lower-level estimator, GOPA-RUE flexibly incorporates reference utility structures and moment-type preference constraints, admits closed-form or semi-closed-form solutions, and remains computationally tractable. The resulting weights decompose explicitly into rank-reciprocal components and reconstructed utilities, offering a unified interpretation of OPA and its generalization. Sensitivity, ablation, and perturbation analyses show that GOPA-RUE is locally responsive yet globally robust: dominance structures remain stable under moderate noise, while nonlinear utility curvature can be accommodated. The emergency supplier selection case further demonstrates applicability in data-scarce and time-critical settings. Overall, the study advances ordinal decision modeling by integrating rank-based weighting with entropy-based utility reconstruction, providing a theoretically grounded and behaviorally flexible framework for decision making under incomplete preference information.

Several limitations suggest directions for future research. First, the study focuses on model formulation and analysis and does not develop efficient procedures for eliciting reference utility structures and moment-type preferences; advances in preference elicitation from finance and behavioral economics may strengthen GOPA in this regard. Second, in large-scale decision contexts, expert preferences may be modeled as realizations of uncertain parameters. Integrating machine learning, contextual optimization, and distributionally robust optimization could offer a promising extension of the GOPA framework.

Appendix A: Technical Proofs

Appendix A.1: Proof of Proposition 1

Consider the inequality system of OPA-I after mapping the alternative index to the rank index r:

$$z \le t_i s_{ij} r(\bar{w}_{ijr} - \bar{w}_{ij,r+1}), \qquad r = 1, \ldots, R-1, \tag{A.1a}$$
$$z \le t_i s_{ij} r \bar{w}_{ijr}, \qquad r = R. \tag{A.1b}$$

Taking the cumulative sum of the last r inequalities in Equation (A.1) yields

$$\left(\sum_{h=r}^{R} \frac{1}{h}\right) z \le t_i s_{ij} \bar{w}_{ijr}, \quad \forall (i, j, r) \in \mathcal{Y}, \tag{A.2}$$

which coincides with the inequality constraints in OPA-II.

The feasible set of OPA-I is nonempty and compact, and the objective function is bounded above. Hence, an optimal solution exists. Moreover, under $t_i s_{ij} > 0$ for all $(i, j, r) \in \mathcal{Y}$, Slater's condition holds and the Karush-Kuhn-Tucker (KKT) conditions are both necessary and sufficient for optimality.

At an optimal solution, all inequalities in Equation (A.1) must be active; otherwise, a strictly larger objective value z could be achieved, contradicting optimality. Consequently, the inequality systems Equations (A.1) and (A.2) are equivalent at optimality, establishing the equivalence between OPA-I and OPA-II. Finally, since the active constraints together with the normalization condition form a full-rank system, the optimal value is unique. □

Appendix A.2: Proof of Theorem 1

Let $F = u_{ij}(x) \ln\big(u_{ij}(x)/v_{ij}(x)\big)$, $G_0 = u_{ij}(x)$, and $G_{b_{ij}} = \phi_{b_{ij}}(x) u_{ij}(x)$ for all $b_{ij} \in \mathcal{B}_{ij}$. Define the auxiliary functional as follows:

$$\begin{aligned} J^* &= \int_0^R F + \lambda_0 G_0 + \sum_{b_{ij} \in \mathcal{B}_{ij}} \lambda_{b_{ij}} G_{b_{ij}} \mathrm{d}x \\ &= \int_0^R u_{ij}(x) \ln\left(\frac{u_{ij}(x)}{v_{ij}(x)}\right) + \lambda_0 u_{ij}(x) + \sum_{b_{ij} \in \mathcal{B}_{ij}} \lambda_{b_{ij}} \phi_{b_{ij}}(x) u_{ij}(x) \mathrm{d}x, \end{aligned}$$

with the Euler equation:

$$\ln\left(\frac{u_{ij}(x)}{v_{ij}(x)}\right) + 1 + \lambda_0 + \sum_{b_{ij} \in \mathcal{B}_{ij}} \lambda_{b_{ij}} \phi_{b_{ij}}(x) = 0.$$

Rearranging the Euler equation provides the optimal solution to the minimum relative utility entropy:

$$u_{ij}^*(x) = v_{ij}(x)e^{-1-\lambda_0-\sum_{b_{ij}\in\mathcal{B}_{ij}}\lambda_{b_{ij}}\phi_{b_{ij}}(x)},$$

which gives the results in Theorem 1. Note that $\phi_{b_{ij}}$ is a step function with jumps at $r_{c_{ij}}$ for all $c_{ij} \in \mathcal{C}_{ij}$ related to the partial preference constraints of deterministic utility comparisons in GOPA. Thus, u_{ij}^* is a piecewise function with breakpoints at $r_{c_{ij}}$ for all $c_{ij} \in \mathcal{C}_{ij}$. □

Appendix A.3: Proof of Corollary 1

Corollary 1 follows directly from Theorem 1. □

Appendix A.4: Proof of Proposition 2

Solving the Euler-Lagrange operators involves substituting the optimal marginal utility density function in Theorem 1 into the constraints of the lower-level problem of GOPA-RUE. It is easy to verify that the system of equations is full rank with dimensions $B_{ij} + 1$.

For any $(i, j) \in \bar{\mathcal{X}}$, define the utility increment as

$$\Delta U_{c_{ij}} = \int_0^{r_{c_{ij}}} u(x)\mathrm{d}x - \int_0^{r_{c_{ij}-1}} u(x)\mathrm{d}x = e^{-1-\lambda_0-\sum_{b_{ij}\in\mathcal{B}_{ij}}\lambda_{b_{ij}}\phi_{b_{ij}}(r_{c_{ij}})} \int_{r_{c_{ij}-1}}^{r_{c_{ij}}} v_{ij}(x)\mathrm{d}x, \quad \forall c_{ij} \in \mathcal{C}_{ij},$$

and $\boldsymbol{\Delta U}_{ij} = (\Delta U_1, \ldots, \Delta U_{C_{ij}})^{\mathrm{T}}$, dependent on $(\lambda_0, \boldsymbol{\lambda})$. The marginal utility functions can be rewritten with the utility increments as

$$U_{ij}(x) = \sum_{c_{ij}\in\mathcal{C}_{ij}} \left(\int_{r_{c_{ij}-1}}^{x} u(x)\mathrm{d}x + \sum_{c'_{ij}=1}^{c_{ij}} \Delta U_{c'_{ij}} \right) \mathbf{1}\left\{x \in (r_{c_{ij}-1}, r_{c_{ij}}]\right\}, \quad \forall (i, j) \in \bar{\mathcal{X}}.$$

Define

$$\Delta V_{c_{ij}} = \int_{r_{c_{ij}-1}}^{r_{c_{ij}}} v_{ij}(x)\mathrm{d}x,$$

$$g_{c_{ij}} = e^{-1-\lambda_0-\sum_{b_{ij}\in\mathcal{B}_{ij}}\lambda_{b_{ij}}\phi_{b_{ij}}(r_{c_{ij}})},$$

for all $c_{ij} \in \mathcal{C}_{ij}$ and $(i, j) \in \bar{\mathcal{X}}$. Let $\boldsymbol{g}_{ij} = (g_1, \ldots, g_{C_{ij}})^{\mathrm{T}}$ and

$$\boldsymbol{\Delta V}_{ij} = \begin{bmatrix} \Delta V_1 & & \\ & \ddots & \\ & & \Delta V_{C_{ij}} \end{bmatrix}.$$

Then, we have the vector of utility increments $\boldsymbol{\Delta U}_{ij}$:

$$\boldsymbol{\Delta U}_{ij} = \boldsymbol{\Delta V}_{ij}\boldsymbol{g}_{ij},$$

where $\boldsymbol{\Delta V}_{ij}$ is the vector of known parameters and $\boldsymbol{g}_{ij}$ is the vector of variables to be solved, consisting of Euler-Lagrange operators.

Next, we construct the coefficient matrix for the constraints. Recall that $\phi_{b_{ij}}(x) = \mathbf{1}_{(0,r_{b_{ij}}]}(x) - \alpha\mathbf{1}_{(0,r_{b'_{ij}}]}(x)$ for all $(i, j) \in \bar{\mathcal{X}}$ and $b_{ij} \in \mathcal{B}_{ij}$. Define

$$\bar{\boldsymbol{\phi}}_{b_{ij}} = \left(\mathbf{1}\left\{r_{b_{ij}} \in (r_1, +\infty)\right\}, \ldots, \mathbf{1}\left\{r_{b_{ij}} \in (r_{C_{ij}}, +\infty)\right\}\right)^{\mathrm{T}},$$

and $\boldsymbol{\beta}_{ij} = (\beta_1, \ldots, \beta_{B_{ij}}, 1)^{\mathrm{T}}$. The coefficient matrix for the constraints is

$$\boldsymbol{\Psi}_{ij} = (\boldsymbol{\psi}_1, \ldots, \boldsymbol{\psi}_{B_{ij}}, \boldsymbol{e})^{\mathrm{T}},$$

where $\boldsymbol{\psi}_{b_{ij}} = \bar{\boldsymbol{\phi}}_{b_{ij}} - \alpha_{b_{ij}} \bar{\boldsymbol{\phi}}_{b'_{ij}}$ and $\boldsymbol{e}$ is a C_{ij}-dimensional vector of all ones for all $(i, j) \in \bar{\mathcal{X}}$. Thus, we need to solve the following system of equations:

$$\boldsymbol{\Psi}_{ij} \boldsymbol{\Delta V}_{ij} \boldsymbol{g}_{ij} = \boldsymbol{\beta}_{ij}.$$

Thus, using the indicator function, the optimal marginal utility density function is given by

$$u^*_{ij}(x) = \sum_{c_{ij} \in \mathcal{C}_{ij}} g^*_{c_{ij}} v_{ij}(x) \mathbf{1}\left\{x \in (r_{c_{ij}-1}, r_{c_{ij}}]\right\},$$

which yields the results in Proposition 2. □

Appendix A.5: Proof of Lemma 1

Fix any $(i, j) \in \bar{\mathcal{X}}$. Recall from Proposition 2 that

$$\boldsymbol{A}_{ij} = \boldsymbol{\Psi}_{ij} \boldsymbol{\Delta} V_{ij},$$

where $\boldsymbol{\Delta} V_{ij}$ is a diagonal matrix with strictly positive diagonal elements and $\boldsymbol{\Psi}_{ij} \in \mathbb{R}^{(B_{ij}+1)\times C_{ij}}$ is constructed from the elicited deterministic comparisons together with the normalization constraint.

We first note that $\boldsymbol{\Delta} V_{ij}$ is nonsingular. Hence,

$$\mathrm{rank}(\boldsymbol{A}_{ij}) = \mathrm{rank}(\boldsymbol{\Psi}_{ij} \boldsymbol{\Delta} V_{ij}) = \mathrm{rank}(\boldsymbol{\Psi}_{ij}),$$

and it suffices to show that $\boldsymbol{\Psi}_{ij}$ has full column rank.

Under the preference elicitation strategy specified in Section 4.2.2, the breakpoint set is induced incrementally from the elicited comparisons. The first comparison may introduce two breakpoints, while each subsequent comparison introduces at most one new breakpoint. As a result, the number of induced segments satisfies $C_{ij} \leq B_{ij} + 1$, so that $\boldsymbol{\Psi}_{ij}$ has at least as many rows as columns. Moreover, each newly introduced breakpoint is associated with at least one comparison whose other endpoint belongs to the existing breakpoint set. Consequently, each new column of $\boldsymbol{\Psi}_{ij}$ corresponding to an induced segment contributes a linearly independent direction relative to the previously constructed columns. Together with the normalization row, this incremental construction ensures that no column of $\boldsymbol{\Psi}_{ij}$ can be expressed as a linear combination of the others.

Therefore, $\boldsymbol{\Psi}_{ij}$ has full column rank, i.e., $\mathrm{rank}(\boldsymbol{\Psi}_{ij}) = C_{ij}$. It follows that

$$\mathrm{rank}(\boldsymbol{A}_{ij}) = C_{ij}.$$

Since $\boldsymbol{A}_{ij}$ has full column rank, the Gram matrix $\boldsymbol{A}_{ij}^{\mathsf{T}} \boldsymbol{A}_{ij}$ is symmetric positive definite and hence nonsingular, which gives the results in Lemma 1. □

Appendix A.6: Proof of Proposition 3

Fix any $(i, j) \in \bar{\mathcal{X}}$ and consider the unconstrained regularized least-squares problem:

$$\min_{\boldsymbol{g}_{ij}} \frac{1}{2} \left\| \boldsymbol{A}_{ij} \boldsymbol{g}_{ij} - \boldsymbol{\beta}_{ij} \right\|_2^2 + \frac{\lambda}{2} \left\| \boldsymbol{g}_{ij} \right\|_2^2.$$

The objective function is continuously differentiable and strictly convex in $\boldsymbol{g}_{ij}$. Hence, the problem admits a unique global minimizer, which is characterized by the first-order optimality condition.

Taking the gradient of the objective function with respect to $\boldsymbol{g}_{ij}$ yields

$$\nabla_{\boldsymbol{g}_{ij}} = \boldsymbol{A}_{ij}^{\top}\left(\boldsymbol{A}_{ij}\boldsymbol{g}_{ij} - \boldsymbol{\beta}_{ij}\right) + \lambda \boldsymbol{g}_{ij}.$$

Setting the gradient equal to zero gives the normal equation:

$$\left(\boldsymbol{A}_{ij}^{\top}\boldsymbol{A}_{ij} + \lambda \boldsymbol{I}\right)\boldsymbol{g}_{ij} = \boldsymbol{A}_{ij}^{\top}\boldsymbol{\beta}_{ij}.$$

By Lemma 1, $\boldsymbol{A}_{ij}$ has full column rank, which implies that $\boldsymbol{A}_{ij}^{\top}\boldsymbol{A}_{ij}$ is symmetric positive definite. Since $\lambda > 0$, the matrix $\boldsymbol{A}_{ij}^{\top}\boldsymbol{A}_{ij} + \lambda \boldsymbol{I}$ is also symmetric positive definite and therefore nonsingular. Consequently, the normal equation admits a unique solution given by

$$\boldsymbol{g}_{ij}^{*} = \left(\boldsymbol{A}_{ij}^{\top}\boldsymbol{A}_{ij} + \lambda \boldsymbol{I}\right)^{-1}\boldsymbol{A}_{ij}^{\top}\boldsymbol{\beta}_{ij}.$$

This solution is the unique global minimizer of the regularized least-squares problem, which gives the results in Proposition 3. □

Appendix A.7: Proof of Corollary 2

For any $(i, j) \in \bar{\mathcal{X}}$, taking the logarithm of the optimal marginal utility density function in Theorem 1 over the breakpoint interval $(r_{c_{ij}-1}, r_{c_{ij}}]$ yields

$$\ln(u_{ij}^{*}(x)) = \ln(v_{ij}(x)) - 1 - \lambda_0 - \sum_{b_{ij} \in \mathcal{B}_{ij}} \lambda_{b_{ij}} \phi_{b_{ij}}(x), \quad x \in (r_{c_{ij}-1}, r_{c_{ij}}], \forall c_{ij} \in \mathcal{C}_{ij},$$

where $\phi_{b_{ij}}(x)$ is a step function, composed of indicator functions.

By Arrow-Pratt's definition of the risk preference function, we obtain the risk preference function for the optimal marginal utility density function with minimum relative utility entropy within each breakpoint interval:

$$\eta_{ij}(x) = -\frac{\mathrm{d}}{\mathrm{d}x}\ln(u_{ij}^{*}(x)) = -\frac{\mathrm{d}}{\mathrm{d}x}\ln(v_{ij}(x)), \quad x \in (r_{c_{ij}-1}, r_{c_{ij}}], \forall c_{ij} \in \mathcal{C}_{ij},$$

which is aligned with the risk preference of the reference utility density function over each interval.

We can further express the risk preference function of the lower-level problem of GOPA-RUE using indicator functions as

$$\eta_{ij}(x) = \sum_{c_{ij} \in \mathcal{C}_{ij}} \left(-\frac{\mathrm{d}}{\mathrm{d}x}\ln(v(x))\right) \mathbf{1}\left\{x \in (r_{c_{ij}-1}, r_{c_{ij}}]\right\}, \quad \forall x \in (0, R].$$

which gives the results in Corollary 2. □

Appendix A.8: Proof of Theorem 2

Let $\lambda_0 \in \mathbb{R}$ and $\boldsymbol{\lambda} \in \mathbb{R}^{\mathcal{Y}}$. By applying the Lagrange multiplier method, we obtain

$$\begin{aligned} L(z, \bar{\boldsymbol{w}}, \lambda_0, \boldsymbol{\lambda}) &= z + \lambda_0 \left(1 - \sum_{i \in \mathcal{I}} \sum_{j \in \mathcal{J}} \sum_{r \in \mathcal{R}} \bar{w}_{ijr}\right) + \sum_{i \in \mathcal{I}} \sum_{j \in \mathcal{J}} \sum_{r \in \mathcal{R}} \lambda_{ijr} \left(RU^*_{ijr} z - t_i s_{ij} \bar{w}_{ijr}\right), \\ &= \lambda_0 + \left(1 + R \sum_{i \in \mathcal{I}} \sum_{j \in \mathcal{J}} \sum_{r \in \mathcal{R}} U^*_{ijr} \lambda_{ijr}\right) z - \sum_{i \in \mathcal{I}} \sum_{j \in \mathcal{J}} \sum_{r \in \mathcal{R}} \left(\lambda_0 + t_i s_{ij} \lambda_{ijr}\right) \bar{w}_{ijr}, \end{aligned}$$

where the constraints $U^*_{ijr} = \int_0^{R-r+1} u^*_{ij}(x)\mathrm{d}x$ for all $(i, j, r) \in \mathcal{Y}$ are not considered because they contain no variables. The upper-level problem of GOPA-RUE is a typical linear optimization problem with the coefficient matrix being full rank. This implies that any set of solutions meeting the KKT condition is an optimal solution and it is unique. Let $(z^*, \bar{\boldsymbol{w}}^*, \lambda_0^*, \boldsymbol{\lambda}^*)$ represent the optimal solution. The KKT condition is as follows:

$$\nabla_z L(z^*, \bar{\boldsymbol{w}}^*, \lambda_0^*, \boldsymbol{\lambda}^*) = 1 + R \sum_{i \in \mathcal{I}} \sum_{j \in \mathcal{J}} \sum_{r \in \mathcal{R}} U^*_{ijr} \lambda_{ijr} = 0, \tag{A.3a}$$

$$\nabla_{\bar{w}_{ijr}} L(z^*, \bar{\boldsymbol{w}}^*, \lambda_0^*, \boldsymbol{\lambda}^*) = \lambda_0 + t_i s_{ij} \lambda_{ijr} = 0, \quad \forall (i, j, r) \in \mathcal{Y}, \tag{A.3b}$$

$$\lambda_{ijr} \left(RU^*_{ijr} z^* - t_i s_{ij} \bar{w}^*_{ijr}\right) = 0, \quad \forall (i, j, r) \in \mathcal{Y}, \tag{A.3c}$$

$$RU^*_{ijr} z^* - t_i s_{ij} \bar{w}^*_{ijr} \leq 0, \quad \forall (i, j, r) \in \mathcal{Y}, \tag{A.3d}$$

$$1 - \sum_{i \in \mathcal{I}} \sum_{j \in \mathcal{J}} \sum_{r \in \mathcal{R}} \bar{w}^*_{ijr} = 0, \tag{A.3e}$$

$$\lambda_{ijr} \leq 0, \quad \forall (i, j, r) \in \mathcal{Y}. \tag{A.3f}$$

Let all constraints in Equation (A.3d) be active and substitute them into Equation (A.3e). Then we have

$$\sum_{i \in \mathcal{I}} \sum_{j \in \mathcal{J}} \sum_{r \in \mathcal{R}} \frac{RU^*_{ijr}}{t_i s_{ij}} z^* = 1,$$

and

$$w^*_{ijr} = \frac{RU^*_{ijr} z^*}{t_i s_{ij}}, \quad \forall (i, j, r) \in \mathcal{Y}.$$

It is straightforward to verify that Equations (A.3a), (A.3b), (A.3c), and (A.3f) are satisfied. Hence, rearranging the above equations yields the optimal solutions in Theorem 2. □

Appendix A.9: Proof of Corollary 3

Given the optimal GOPA-RUE weights in Theorem 2 and

$$\bar{z}^* = \left(\sum_{i \in \mathcal{I}} \sum_{j \in \mathcal{J}} \frac{R}{t_i s_{ij}}\right)^{-1},$$

for any $(i, j, r) \in \mathcal{Y}$, we have

$$\bar{w}_{ijr}^{*} = \frac{RU_{ijr}^{*} z^{*}}{t_i s_{ij}} = \frac{RU_{ijr}^{*} \bar{z}^{*}}{t_i s_{ij}} \left(\frac{z^{*}}{\bar{z}^{*}}\right) = \frac{1}{t_i s_{ij} \sum_{i \in \mathcal{I}} \sum_{j \in \mathcal{J}} \frac{1}{t_i s_{ij}}} \left(\frac{z^{*}}{\bar{z}^{*}} U_{ijr}^{*}\right) = w_{t_i}^{RR} w_{s_{ij}}^{RR} \left(\frac{z^{*}}{\bar{z}^{*}} U_{ijr}^{*}\right).$$

Let $w_{ijr}^{MRU} = \frac{z^{*}}{\bar{z}^{*}} U_{ijr}^{*}$. We have:

$$\sum_{i \in \mathcal{I}} \sum_{j \in \mathcal{J}} \sum_{r \in \mathcal{R}} w_{ijr}^{MRU} = \sum_{i \in \mathcal{I}} \sum_{j \in \mathcal{J}} \sum_{r \in \mathcal{R}} \left(U_{ijr}^{*} \left(\sum_{i \in \mathcal{I}} \sum_{j \in \mathcal{J}} \frac{R}{t_i s_{ij}} \right) \Big/ \sum_{i \in \mathcal{I}} \sum_{j \in \mathcal{J}} \sum_{r \in \mathcal{R}} \frac{RU_{ijr}^{*}}{t_i s_{ij}} \right) = 1.$$

Furthermore, it is clear that $w_{ijr}^{MRU} > w_{ijr+1}^{MRU}$ since $U_{ijr}^{*} > U_{ijr+1}^{*}$ for $r = 1, \ldots, R-1$ and $(i, j) \in \bar{\mathcal{X}}$. □

Appendix A.10: Proof of Theorem 3

Let $(\lambda_0^{*}, \boldsymbol{\lambda}^{*})$ denote the dual optimal solution, i.e.,

$$\begin{aligned}
(\lambda_0^{*}, \boldsymbol{\lambda}^{*}) = \arg \min_{\lambda_0, \boldsymbol{\lambda}} \ & \lambda_0, \\
\text{s.t. } & t_i s_{ij} \lambda_{ijr} \leq \lambda_0, && \forall (i, j, r) \in \mathcal{Y}, \\
& \sum_{i \in \mathcal{I}} \sum_{j \in \mathcal{J}} \sum_{r \in \mathcal{R}} RU_{ijr}^{*} \lambda_{ijr} = 1, \\
& \lambda_{ijr} \geq 0, && \forall (i, j, r) \in \mathcal{Y}.
\end{aligned}$$

Assume that $(z, \bar{\boldsymbol{w}})$ is feasible for the constraint perturbation problem. By strong duality, we have

$$\begin{aligned}
z^{*} &\geq z + \lambda_0^{*} \left(1 - \sum_{i \in \mathcal{I}} \sum_{j \in \mathcal{J}} \sum_{r \in \mathcal{R}} \bar{w}_{ijr}\right) + \sum_{i \in \mathcal{I}} \sum_{j \in \mathcal{J}} \sum_{r \in \mathcal{R}} \lambda_{ijr}^{*} \left(t_i s_{ij} \bar{w}_{ijr} - RU_{ijr}^{*} z\right), \\
&\geq z + \lambda_0^{*} \epsilon + \sum_{i \in \mathcal{I}} \sum_{j \in \mathcal{J}} \sum_{r \in \mathcal{R}} \lambda_{ijr}^{*} \varepsilon_{ijr},
\end{aligned}$$

where the last inequality follows from the constraints in the perturbation problem and $\lambda_{ijr}^{*} \geq 0$ for all $(i, j, r) \in \mathcal{Y}$.

For any feasible z in the perturbation problem, we have

$$z \leq z^{*} - \lambda_0^{*} \epsilon - \sum_{i \in \mathcal{I}} \sum_{j \in \mathcal{J}} \sum_{r \in \mathcal{R}} \lambda_{ijr}^{*} \varepsilon_{ijr},$$

which implies

$$z^{*}(\boldsymbol{\varepsilon}, \epsilon) \leq z^{*} - \lambda_0^{*} \epsilon - \sum_{i \in \mathcal{I}} \sum_{j \in \mathcal{J}} \sum_{r \in \mathcal{R}} \lambda_{ijr}^{*} \varepsilon_{ijr}.$$

Let $\sigma_{ijr} = RU_{ijr}^{*} \lambda_{ijr}$ for all $(i, j, r) \in \mathcal{Y}$. Following the symmetric arguments as in the proof of Theorem 2, we obtain

$$\lambda_0^{*} = \left(\sum_{i \in \mathcal{I}} \sum_{j \in \mathcal{J}} \sum_{r \in \mathcal{R}} \frac{RU_{ijr}^{*}}{t_i s_{ij}} \right)^{-1} = z^{*},$$

and

$$\sigma^*_{ijr} = \frac{RU^*_{ijr}\lambda^*_0}{t_i s_{ij}} \Leftrightarrow \lambda^*_{ijr} = \frac{\lambda^*_0}{t_i s_{ij}}, \quad \forall (i, j, r) \in \mathcal{Y}.$$

Thus, we have

$$\begin{aligned} z^*(\boldsymbol{\varepsilon}, \epsilon) &\leq z^* - \varepsilon_{ijr} z^* - \sum_{i \in \mathcal{I}} \sum_{j \in \mathcal{J}} \sum_{r \in \mathcal{R}} \frac{\varepsilon_{ijr}}{t_i s_{ij}} z^*, \\ &= \left(1 - \varepsilon_{ijr} - \sum_{i \in \mathcal{I}} \sum_{j \in \mathcal{J}} \sum_{r \in \mathcal{R}} \frac{\varepsilon_{ijr}}{t_i s_{ij}} \right) z^*, \end{aligned}$$

which provides the upper bound in Theorem 3. □

Appendix A.11: Proof of Corollary 4

Let $\tau_{ij} = t_i s_{ij} + \sigma_{ij}$ for all $(i, j) \in \bar{\mathcal{X}}$ and $\mu_{ijr} = U^*_{ijr} + \delta_{ijr}$ for all $(i, j, r) \in \mathcal{Y}$. Using symmetric arguments as in the proof of Theorem 2, we derive

$$z^* = \left(\sum_{i \in \mathcal{I}} \sum_{j \in \mathcal{J}} \sum_{r \in \mathcal{R}} \frac{R\mu_{ijr}}{\tau_{ij}} \right)^{-1},$$

and

$$\bar{w}^*_{ijr} = \frac{R\mu_{ijr} z^*}{\tau_{ij}}, \quad \forall (i, j, r) \in \mathcal{Y}.$$

Substituting the expressions for τ_{ij} and μ_{ijr} leads to the results in Corollary 4. □

Acknowledgements This research did not receive any specific grant from funding agencies in the public, commercial, or not-for-profit sectors.

Data Availability Data will be made available on request.

Declarations

Competing interests The authors declare that they have no known competing financial interests or personal relationships that could have appeared to influence the work reported in this paper.

References

Abbas, A. E. (2006). Maximum entropy utility. *Operations Research, 54*, 277–290. https://doi.org/10.1287/opre.1040.0204

Ahn, B. S. (2015). Extreme point-based multi-attribute decision analysis with incomplete information. *European Journal of Operational Research,240*, 748–755. https://doi.org/10.1016/j.ejor.2014.07.037

Ahn, B. S. (2017). Approximate weighting method for multiattribute decision problems with imprecise parameters. *Omega, 72*, 87–95. https://doi.org/10.1016/j.omega.2016.11.006

Ahn, B. S. (2024). Solving multi-attribute decision making problems with incomplete weights: A dual approach. *Journal of the Operational Research Society, 75*, 888–895. https://doi.org/10.1080/01605682.2023.2217212

Armbruster, B., & Delage, E. (2015). Decision making under uncertainty when preference information is incomplete. *Management Science, 61*, 111–128. https://doi.org/10.1287/mnsc.2014.2059

Ataei, Y., Mahmoudi, A., Feylizadeh, M. R., & Li, D. F. (2020). Ordinal priority approach (OPA) in multiple attribute decision-making. *Applied Soft Computing, 86*, Article 105893. https://doi.org/10.1016/j.asoc.2019.105893

Burk, R. C., & Nehring, R. M. (2023). An empirical comparison of rank-based surrogate weights in additive multiattribute decision analysis. *Decision Analysis, 20*, 55–72. https://doi.org/10.1287/deca.2022.0456
Chen, L., & Sim, M. (2024). Robust CARA optimization. *Operations Research*. https://doi.org/10.1287/opre.2021.0654
Cui, S., Wang, R., Li, X., & Bai, X. (2025). Policy-driven analysis of carbon emission efficiency under uncertainty and its application in chinese industry: Hybrid delta-slacks-based model and ordinal priority approach. *Energy, 324*, Article 135832. https://doi.org/10.1016/j.energy.2025.135832
Cui, S., Zhu, F., & Wang, R. (2025). Nuclear energy technology R&D portfolio selection under scenario uncertainty: Distributionally robust ordinal priority approach. *Energy, 337*, Article 138512. https://doi.org/10.1016/j.energy.2025.138512
Du, J. L., Liu, S. F., Javed, S. A., Goh, M., & Chen, Z. S. (2023). Enhancing quality function deployment through the integration of rough set and ordinal priority approach: A case study in electric vehicle manufacturing. *IEEE Transactions on Engineering Management, 71*, 7541–7552. https://doi.org/10.1109/TEM.2023.3282228
Greco, S., Mousseau, V., & Słowiński, R. (2008). Ordinal regression revisited: Multiple criteria ranking using a set of additive value functions. *European Journal of Operational Research, 191*, 416–436. https://doi.org/10.1016/j.ejor.2007.08.013
Jose, V. R. R., Nau, R. F., & Winkler, R. L. (2008). Scoring rules, generalized entropy, and utility maximization. *Operations Research, 56*, 1146–1157. https://doi.org/10.1287/opre.1070.0498
Kim, S. H., & Ahn, B. S. (1999). Interactive group decision making procedure under incomplete information. *European Journal of Operational Research, 116*, 498–507. https://doi.org/10.1016/S0377-2217(98)00040-X
Kucuksari, S., Pamucar, D., Deveci, M., Erdogan, N., & Delen, D. (2023). A new rough ordinal priority-based decision support system for purchasing electric vehicles. *Information Sciences, 647*, Article 119443. https://doi.org/10.1016/j.ins.2023.119443
Liesiö, J., Kallio, M., & Argyris, N. (2023). Incomplete risk-preference information in portfolio decision analysis. *European Journal of Operational Research, 304*, 1084–1098. https://doi.org/10.1016/j.ejor.2022.04.043
Llamazares, B. (2024). Ranking voting systems and surrogate weights: Explicit formulas for centroid weights. *European Journal of Operational Research, 317*, 967–976. https://doi.org/10.1016/j.ejor.2024.04.021
Mahmoudi, A., Abbasi, M., & Deng, X. (2022). A novel project portfolio selection framework towards organizational resilience: Robust ordinal priority approach. *Expert Systems with Applications, 188*, Article 116067. https://doi.org/10.1016/j.eswa.2021.116067
Mahmoudi, A., Abbasi, M., Yuan, J., & Li, L. (2022). Large-scale group decision-making (LSGDM) for performance measurement of healthcare construction projects: Ordinal priority approach. *Applied Intelligence, 52*, 13781–13802. https://doi.org/10.1007/s10489-022-04094-y
Mahmoudi, A., Deng, X., Javed, S. A., & Zhang, N. (2021). Sustainable supplier selection in megaprojects: Grey ordinal priority approach. *Business Strategy and the Environment, 30*, 318–339. https://doi.org/10.1002/bse.2623
Mahmoudi, A., & Javed, S. A. (2022). Probabilistic approach to multi-stage supplier evaluation: Confidence level measurement in ordinal priority approach. *Group Decision and Negotiation, 31*, 1051–1096. https://doi.org/10.1007/s10726-022-09790-1
Malakooti, B. (2000). Ranking and screening multiple criteria alternatives with partial information and use of ordinal and cardinal strength of preferences. *IEEE Transactions on Systems, Man, and Cybernetics-Part A: Systems and Humans, 30*, 355–368. https://doi.org/10.1109/3468.844359
Mao, H., & Wang, R. (2026). Robust consensus ordinal priority approach for improvisational emergency supplier selection under expert consensus ambiguity. *Scientific Reports*. https://doi.org/10.1038/s41598-026-36876-6
Pamucar, D., Deveci, M., Gokasar, I., Tavana, M., & Köppen, M. (2022). A metaverse assessment model for sustainable transportation using ordinal priority approach and Aczel-Alsina norms. *Technological Forecasting and Social Change, 182*, Article 121778. https://doi.org/10.1016/j.techfore.2022.121778
Peng, C., & Delage, E. (2024). Data-driven optimization with distributionally robust second order stochastic dominance constraints. *Operations Research, 72*, 1298–1316. https://doi.org/10.1287/opre.2022.2387
Peng, J., & Zhang, J. (2022). Urban flooding risk assessment based on gis-game theory combination weight: A case study of zhengzhou city. *International Journal of Disaster Risk Reduction, 77*, Article 103080. https://doi.org/10.1016/j.ijdrr.2022.103080
Resende, C. H. L., Lima-Junior, F. R., & Carpinetti, L. C. R. (2023). Decision-making models for formulating and evaluating supplier development programs: A state-of-the-art review and research paths. *Transportation Research Part E: Logistics and Transportation Review, 180*, Article 103340. https://doi.org/10.1016/j.tre.2023.103340

Sadeghi, M., Mahmoudi, A., Deng, X., & Luo, X. (2023). Prioritizing requirements for implementing blockchain technology in construction supply chain based on circular economy: Fuzzy ordinal priority approach. *International Journal of Environmental Science and Technology, 20*, 4991–5012. https://doi.org/10.1007/s13762-022-04298-2

Sütçü, M. (2022). Disutility entropy in multi-attribute utility analysis. *Computers & Industrial Engineering, 169*, Article 108189. https://doi.org/10.1016/j.cie.2022.108189

Timonin, M. (2013). Robust optimization of the Choquet integral. *Fuzzy Sets and Systems, 213*, 27–46. https://doi.org/10.1016/j.fss.2012.04.014

Tversky, A., & Kahneman, D. (1974). Judgment under uncertainty: Heuristics and biases: Biases in judgments reveal some heuristics of thinking under uncertainty. *Science, 185*, 1124–1131. https://doi.org/10.1126/science.185.4157.1124

Wang, R. (2024). A hybrid madm method considering expert consensus for emergency recovery plan selection: Dynamic grey relation analysis and partial ordinal priority approach. *Information Sciences, 677*, Article 120784. https://doi.org/10.1016/j.ins.2024.120784

Wang, R. (2025). Preference robust ordinal priority approach with preference elicitation under incomplete information for multi-attribute robust ranking and selection. https://doi.org/10.48550/arXiv.2412.12690, arXiv:2412.12690.

Wang, R., Shen, R., Cui, S., Shao, X., Chi, H., & Gao, M. (2025). Multi-attribute decision-making approach for improvisational emergency supplier selection: Partial ordinal priority approach. *Expert Systems with Applications, 288*, Article 128196. https://doi.org/10.1016/j.eswa.2025.128196

Wang, R., Wang, E., Li, L., & Li, W. (2022). Evaluating the effectiveness of the COVID-19 emergency outbreak prevention and control based on CIA-ISM. *International Journal of Environmental Research and Public Health, 19*,. https://doi.org/10.3390/ijerph19127146

Wang, Y. M., Chin, K. S., & Yang, J. B. (2007). Three new models for preference voting and aggregation. *Journal of the Operational Research Society, 58*, 1389–1393. https://doi.org/10.1057/palgrave.jors.2602295

Xie, J., Wu, B., & Zou, W. (2024). Ordered weighted utility distance operators and their applications in group decision-making. *Applied Soft Computing, 150*, Article 111016. https://doi.org/10.1016/j.asoc.2023.111016

Zayat, W., Kilic, H. S., Yalcin, A. S., Zaim, S., & Delen, D. (2023). Application of madm methods in industry 4.0: A literature review. *Computers & Industrial Engineering, 177*, Article 109075. https://doi.org/10.1016/j.cie.2023.109075

Zhao, S., Hendalianpour, A., & Liu, P. (2024). Blockchain technology in omnichannel retailing: A novel fuzzy large-scale group-dematel & ordinal priority approach. *Expert Systems with Applications, 249*, Article 123485. https://doi.org/10.1016/j.eswa.2024.123485